AD_____

Award Number: W81XWH-12-1-0460

TITLE: Early Detection of Ovarian Cancer by Tumor Epithelium-Targeted Molecular Ultrasound

PRINCIPAL INVESTIGATOR: Animesh Barua, Ph.D.

CONTRACTING ORGANIZATION: Rush University Medical Center
Chicago, IL 60612

REPORT DATE: October 2014

TYPE OF REPORT: Annual

PREPARED FOR: U.S. Army Medical Research and Materiel Command
Fort Detrick, Maryland 21702-5012

REPORT DOCUMENTATION PAGE

Form Approved
OMB No. 0704-0188

1. REPORT DATE	2. REPORT TYPE	3. DATES COVERED
October 2014	Annual	30 Sep 2013 - 29 Sep 2014

4. TITLE AND SUBTITLE

Early Detection of Ovarian Cancer by Tumor Epithelium-Targeted Molecular Ultrasound

5a. CONTRACT NUMBER

5b. GRANT NUMBER
W81XWH-12-1-0460

5c. PROGRAM ELEMENT NUMBER

6. AUTHOR(S)
Animesh Barua, Ph.D.

E-Mail: Animesh_Barua@rush.edu

5d. PROJECT NUMBER

5e. TASK NUMBER

5f. WORK UNIT NUMBER

7. PERFORMING ORGANIZATION NAME(S) AND ADDRESS(ES)

Rush University Medical Center,
Chicago, IL 60612

8. PERFORMING ORGANIZATION REPORT NUMBER

9. SPONSORING / MONITORING AGENCY NAME(S) AND ADDRESS(ES)
U.S. Army Medical Research and Materiel Command
Fort Detrick, Maryland 21702-5012

10. SPONSOR/MONITOR'S ACRONYM(S)

11. SPONSOR/MONITOR'S REPORT NUMBER(S)

12. DISTRIBUTION / AVAILABILITY STATEMENT
Approved for Public Release; Distribution Unlimited

13. SUPPLEMENTARY NOTES

14. ABSTRACT: The high rate of death of ovarian cancer (OVCA) patients can be prevented if it is detected at early stage. Unfortunately, currently available traditional transvaginal ultrasound (TVUS) imaging together with serum CA-125 levels cannot detect OVCA at early stage. Malignant nuclear transformations followed by the establishment of tumor associated neo-angiogenesis are the early events in tumor development. Ovulation is an inflammatory process which exposes ovarian surface and fimbrial epithelium to inflammatory factors including interleukin 16 (IL-16). Inflammation of the ovary and tubal epithelium due to frequent ovulation leads to the development of oxidative stress and longstanding unresolved oxidative stress causes malignant transformation. Expression of IL-16 by the tumor epithelium and its serum levels has been reported to be increased during OVCA development. Thus IL-16 represents a potential marker of early OVCA which can be detected *in vivo* by ultrasound imaging provided an IL-16-targeted molecular imaging agent can be developed. The goal of this study is to develop and test the efficacy of molecular (IL-16)-targeted ultrasound (MT-U/S) imaging probe for the detection of early OVCA. This goal is being accomplished by two specific aims. Visualization of ovarian tumors in hens by TVUS improved significantly by IL-16-targeted imaging probes (Aim 1). Results obtained so far under Aim-2(Year-2 of the project life) suggest that IL-16-targeted TVUS imaging improved the detection of OVCA at early stage. Monitoring of hens continues to determine the predictability of IL-16-targeted imaging agents for early detection of OVCA.

15. SUBJECT TERMS
Ovarian cancer, Early detection, Molecular-targeted Ultrasound imaging, IL-16, laying hen model

16. SECURITY CLASSIFICATION OF:			17. LIMITATION OF ABSTRACT	18. NUMBER OF PAGES	19a. NAME OF RESPONSIBLE PERSON
a. REPORT	b. ABSTRACT	c. THIS PAGE			USAMRMC
U	U	U	UU	48	19b. TELEPHONE NUMBER *(include area code)*

Table of Contents

Page

INTRODUCTION:

Ovarian cancer (OVCA) is a fatal malignancy of women with high case-to-death ratio of patients [1]. This high rate of death can be prevented can be prevented if it is detected at early stage. Unfortunately, non-specificity of symptoms at early stage and a lack of an effective early detection test, OVCA in most cases is detected at late stages when the 5-year survival rate of patients is <20% as opposed to >80% if detected at early stage [2]. Ovulation is an inflammatory process which exposes ovarian surface (site of ovulatory rupture) and fimbrial epithelium to inflammatory factors including interleukin 16 (IL-16) secreted by immune cells. Inflammation of the ovary and tubal epithelium due to frequent ovulation leads to the development of oxidative stress and longstanding unresolved oxidative stress has been suggested to cause malignant transformation. Malignant nuclear transformations followed by the establishment of tumor associated neo-angiogenesis are the early events in tumor development and progression. During malignant nuclear transformation, the shape and sizes of the nucleus undergo profound changes together with the rearrangement of nuclear matrix proteins (NMP) leading to the shedding of NMPs into the circulation. Anti-NMP antibodies are produced in response to shed NMPs [3, 4]. On the other hand, expression of IL-16 by the tumor epithelium and its serum levels increase in association with ovarian tumor development [5]. Thus IL-16 represents a potential marker of early OVCA which can be detected by ultrasound imaging provided an IL-16-targeted MT-U/S imaging agent can be developed. Approaches involving serum CA-125 levels, traditional transvaginal ultrasound (TVUS) imaging or their combination did not improve the early detection rates of OVCA. Because CA-125 is not specific for early OVCA and the traditional TVUS imaging cannot detect early OVCA due to its limited resolution [6]. Thus current detection limit of traditional TVUS imaging needs to be improved. MT-U/S can detect tumor associated changes expressed by the tumor epithelium or by the endothelium of tumor associated microvessels. The goal of this study is to develop and test the efficacy of IL-16-targeted MT-U/S imaging agent for the detection of early OVCA in association with its serum levels together with serum anti- NMP antibodies. This goal is being achieved by two specific aims. IL-16-targeted MT-U/S imaging agent was developed and tested in Aim-1. Using IL-16-targeted imaging indices established in Aim-1, hens are being monitored prospectively to detect early stage OVCA in Aim-2.

BODY: the research accomplishments associated with Task-2 outlined in the approved Statement of Work (SOW).

The hypothesis of this project is that *OVCA at early stage can be detected using molecular (IL-16) - targeted ultrasound (MT-US) imaging in association with serum IL-16 levels and anti-NMP antibodies.* The approach to test the hypothesis was to develop a tumor targeted (tumor epithelium and tumor-associated microvessels) imaging agent (IL-16) to enhance visualization of tumors and to examine its ability to detect ovarian tumors at early stage. First part of this approach: *development of IL-16-targeted TVUS imaging agent and its ability to enhance the visualization of ovarian tumors* was examined through Task-1 (Aim 1) and included in the Year-1 report submitted previously. The second part of the approach '*determine the detection ability of early stage OVCA by IL-16-targeted TVUS imaging agents in laying hens* is being performed in Task 2 (Aim 2). The work in Year-2 (Task-2) so far been achieved are reported below:

Task 2. Determination of specificity, sensitivity and predictive values of MT-U/S imaging and serum markers diagnostic of OVCA.

2a. Selection of hens for prospective monitoring:

1. Egg rates of hens were examined and hens laying fewer eggs (low egg laying rates as an indicator of decreased ovarian function) were selected based on the prevalence of circulating anti-NMP (ovarian

nuclear matrix protein) antibodies as well as without any ovarian abnormalities detectable by IL-16-targeted TVUS imaging established in Aim-1.

2. Selected hens with (n=50 hens) or without (n=50 hens) serum anti-NMP antibodies are being monitored using IL-16-targted TVUS imaging prospectively described in detail in subsequent sections.

2b. Scanning of hens for the detection of ovarian tumor or TAN by MT-U/S imaging and Optison™ enhanced Doppler ultrasound imaging prospectively:

1. Selected hens were monitored and are being monitored by IL-16-targted TVUS imaging prospectively at 15 weeks with reference to imaging indices detective of ovarian malignant transformation determined in Task 1 (Aim 1).
2. Serum samples were collected at each scan for biochemical assay including the prevalence of anti-NMP antibodies and IL-16 levels.
3. Hens indicated to have early stage ovarian cancer by IL-16-targeted TVUS imaging were sacrificed at the time of diagnosis. Gross evaluation was performed and ovarian tissues were collected and processed for routine histology, immunohistochemical, proteomic and gene expression studies. Presence of tumors and their types were determined.
4. Ovarian tissues were examined for IL-16 expression by the tumor epithelium and the endothelial cells of tumor associated microvessels as well as α-smooth muscle actin (α-SMA) expression.
5. Tissue expression and serum levels of IL-16 were confirmed by Western blotting.
6. One of the reasons of prospective monitoring of hens is to predict the time between a dormant malignant lesion and earliest TVUS detectable ovarian solid mass. Due to individual variation in tumor associated expression of IL-16, the approach is to determine the median time (in weeks) following the prevalence of serum anti-NMP antibodies and the detection of tumor. Thus the length of prospective monitoring of hens needs to be extended to additional 3 months and a request has been submitted to the sponsor for such extension.
7. The predictive value of the diagnostic indices of IL-16-targeted imaging determined in Task 1(Aim 1) will be tested at the end of the Task 2 (Aim 2).

Detailed Reports on the Accomplishments in Year-2 of the project life:

Specific Aim 2: Ovarian MT-U/S imaging indices and angiogenic indices (AI) in hens with anti-NMP antibodies will predict development of OVCA.

Animals: 3-4years old hens with low egg laying rates (<100 eggs/year) were selected from a flock of White Leghorn laying hens. Selected hens were tested for the presence of serum anti-NMP antibodies. 50 hens with anti-NMP antibodies and 50 hens without anti-NMP antibodies were selected for prospective monitoring by IL-16-targeted TVUS imaging for the detection of ovarian tumors using imaging indices established in Specific Aim 1. Hens were maintained and are being maintained in a standard poultry husbandry practices access to food and water *ad libitum*.

Serum: Blood from all selected hens were collected at each scan, serum samples were separated and stored at -80^{o}C to determine the prevalence of anti-NMP antibodies and IL-16 levels by immunoassay later.

Molecular (IL-16) targeted ultrasound imaging and analysis of images:

Traditional ultrasound imaging (pre-targeted): Traditional transvaginal ultrasound (TVUS) imaging was performed prior to the injection of microbubbles containing IL-16-targeted imaging agents using mechanical set up reported earlier[7, 8]. Briefly, hens were held carefully by an assistant and imaging was performed using an instrument attached with a 5- to 7.5-MHz endovaginal transducer (MicroMaxx; SonoSite, Inc, Bothell, WA). Hens were immobilized, the transducer was inserted transvaginally, 2-dimensional transvaginal gray scale and pulsed Doppler sonographies were performed [7, 9]. Examination of ovarian morphology was performed by gray scale TVUS and the vascular network of the ovary were evaluated by Doppler ultrasound (DUS) imaging. Blood flow characteristics including the resistive index (RI: [systolic velocity – diastolic velocity]/systolic velocity) and the pulsatility index (PI: [systolic velocity – diastolic velocity]/mean) were automatically calculated from at least two separate Doppler images from the same ovary as reported earlier [7, 9, 10]. The lower RI and PI values are used for analysis. Images were processed and archived digitally for reviewing off-line later.

IL-16-targeted TVUS imaging:
Molecular targeted ultrasound imaging was performed following pre-targeted imaging. Hens were injected with microbubbles containing IL-16-targeted imaging agents in a similar manner with identical mechanical settings as described above. Ovarian tissues including the same area imaged during pre-targeted scanning were imaged similar to that reported earlier [8]. Microbubbles containing targeted imaging agents were observed to be accumulated in the ovary around 5-7 min from their arrival. Free unbound microbubbles were washed out. All images including still and real-time clips were archived electronically (~ 15 minutes for each hen). Visual evaluation of the effects of targeted imaging agents was performed online (during scanning) and off-line later by reviewing the archived still images and video clips. The time of targeted imaging agent arrival (interval in seconds from administration of the imaging agents to its visual observation [in seconds]) in the ovaries with or without tumor was recorded in real time. The region of interest (ROI) was selected following review of the complete clip. The average image intensity (in arbitrary values) over a ROI containing the tumor or normal ovarian stroma was calculated by computer assisted software (Microsuite^{TM} version Five, Olympus America, Inc., Canter Valley, PA). Diagnosis of OVCA was performed on the basis of targeted ultrasound signal intensities with reference to that determined in specific aim 1. Furthermore, post-targeted RI and PI values were calculated.

Ovarian gross morphology and microscopic observation:
All hens predicted to have OVCA were sacrificed and gross pathology including presence of ovarian solid mass with or without accompanied ascites and tumor metastasis to distant organs was determined as reported earlier [11]. Gross morphology was recorded and photographed by a digital camera. Tissues were processed for routine staining to confirm the presence of tumors and their histological sub-types as reported earlier [11], immunohistochemical studies, immunoblotting as well as gene expression. Paraffin sections were also used to determine histological sub-types of ovarian tumors as well as immunohistochemical and immunoblotting studies as reported previously [11].

Immunoassay and Immunoblotting: Prevalence of anti-NMP antibodies in serum and circulating levels of IL-16 were determined by ELISA and confirmed by 1 & 2-dimensional Western blotting as reported earlier [12, 5]. Similarly, tissue expression of IL-16 was also confirmed by immunoblotting

Immunohistochemistry: Paraffin sections of ovarian tumors were used to examine IL-16 and α-smooth muscle actin (SMA)-expression by the tumor epithelium and the tumor associated microvessels as reported earlier [12, 5]. The frequencies of IL-16-expressing cells as well as microvessels expressing α-SMA and IL-16 were counted and analyzed as reported previously [12, 5]

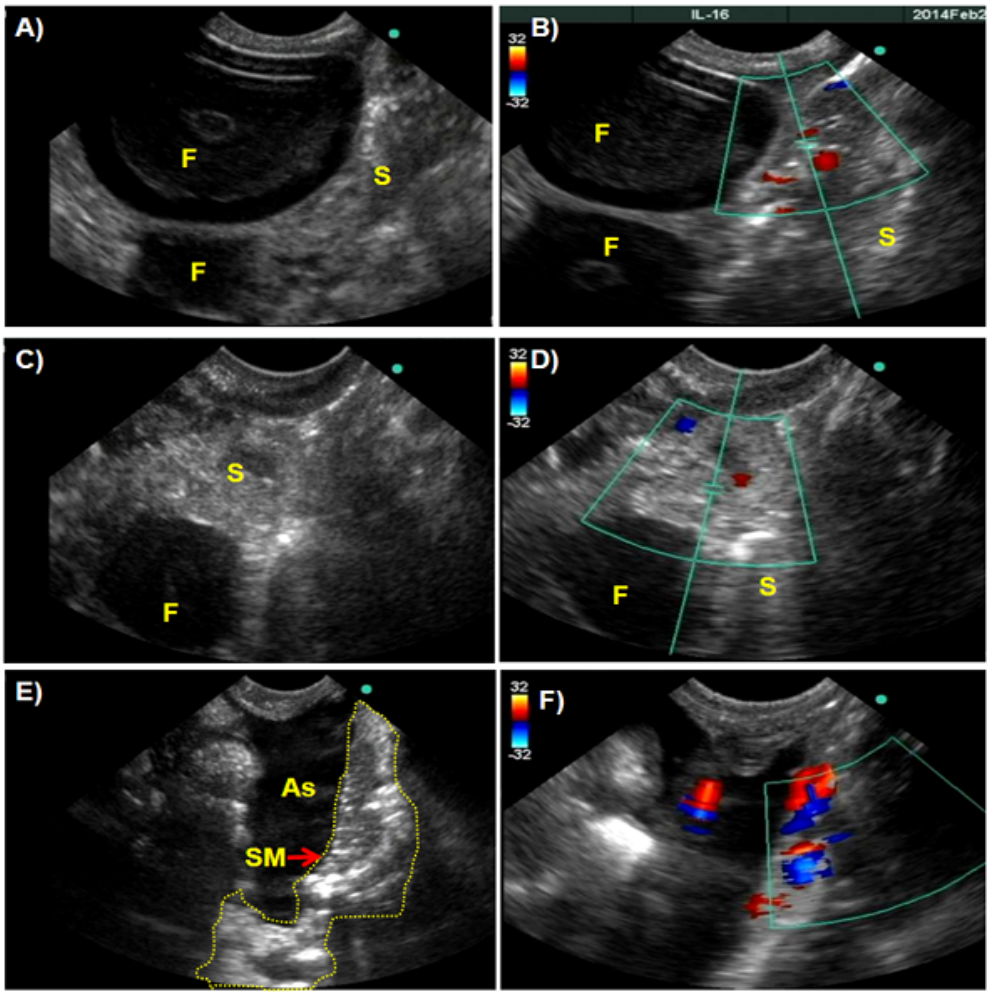

Figure X: Changes in ovarian morphology leading to tumor development in hens detected by prospective IL-16-targeted molecular ultrasound imaging. ***A-B***) Gray scale and Doppler sonogram of a hen ovary at 1st scan showing two developing preovulatory follicles (F) in the stroma (S). No abnormality was detected in gray scale ovarian morphology and in ovarian vasculature by Doppler ultrasound scan. ***C-D***) At 2nd scan (30 weeks after) no remarkable change was observed in the same ovary by gray scale and Doppler sonography except the number of follicles. Compared with 1st scan, the number of developing follicle decreased as the hen ages. ***E-F***) The hen presented in 1st and 2nd scan developed solid mass (SM) and detected by targeted imaging at 3rd scan. Compared with 1st and 2nd scan, more microvessels were detected during 3rd scan by Doppler imaging suggesting tumor associated changes in ovarian blood flow. As=Ascites.

Results:

***Development of tumor associated changes in the ovary and its detection by prospective monitoring using IL-16-targeted TVUS imaging*:** Ovaries in hens with serum anti-NMP antibodies had one or two preovulatory follicles without any abnormal solid mass during at first scan after 15-weeks from the start of the prospective scanning (**Figure 1A-B**). Similarly, remarkable changes in Doppler indices indicative of tumor associated blood flow characteristics were also not observed. In addition, significant increase in serum IL-16 levels was also not recorded. Compared with first scan, serum levels of IL-16 increased at second scan after 30 weeks from initial scan in 11 of 50 hens with anti-NMP antibodies. Compared with 1st scan, significant increase in the intensity of IL-16-targeted imaging was recorded in these hens at second scan after 30 weeks (**Figure 1C-D**). However, tumor associated changes in ovarian morphology were not observed. After 45 weeks from initial scan (3rd scan), tumor associated changes in ovarian morphology including high intensity of IL-16-tergeted imaging (**Figure 1E-F**), serum IL-16 levels and Doppler

indices were observed in 11 hens (**Figure 1F**). Targeted imaging also showed presence ascites-like fluids in few of these hens (3). All these hens were considered to have OVCA.

Gross morphology and microscopic examinations of hens suggested to have ovarian tumors by targeted imaging:

All hens predicted to have ovarian tumors by IL-16-targeted TVUS imaging were sacrificed after imaging. Ovarian gross morphology examined, photographed and compared with ultrasound imaging predictions. Presence of solid tumor mass in the ovary, degree of tumor metastasis, stages of OVCA and accompanying ascites (if any) was recorded. Ovaries with tumor and oviducts were collected, processed for paraffin, frozen, proteomic and molecular biological studies. Routine microscopic examination with hematoxylin-eosin staining were performed to confirm sub-types of ovarian tumors (**Figure 2**) as reported earlier [11]. Gross and histological examinations revealed adenocarcinoma of the ovary and confirmed the predictions of IL-16-targeted TVUS imaging. Of 11 hens, 9 hens had tumors limited to the ovaries (early stage) and 2 hens had tumors metastasized to other organs associated with ascites.

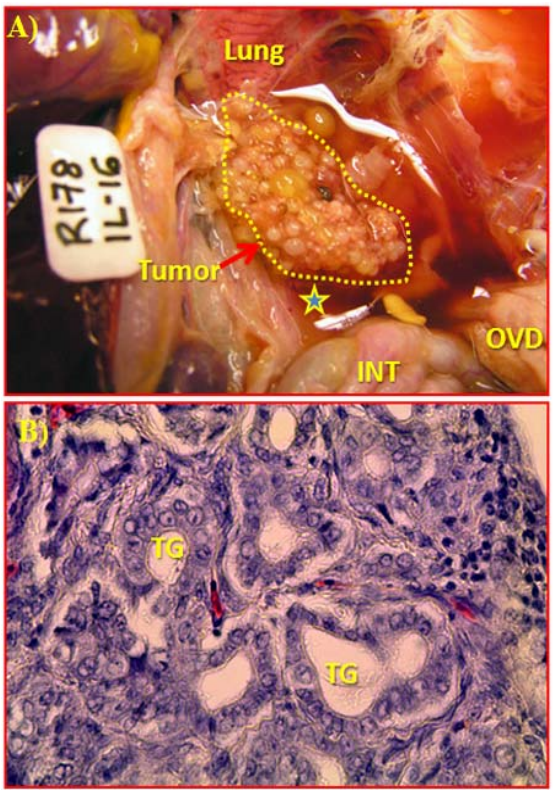

Figure 2: Ovarian tumors at early stage in a hen detected by IL-16-targeted molecular ultrasound imaging presented in *figure 1*. A) Gross presentation of the tumor showing the solid mass limited to the ovary accompanied with little ascites. No metastasis is seen to the other organs including oviduct (OVD) and intestine (INT). B) Routine staining (hematoxylin and eosin) and microscopic examination confirmed the mass is an adenocarcinoma of the ovary. TG=tumor gland. 40X

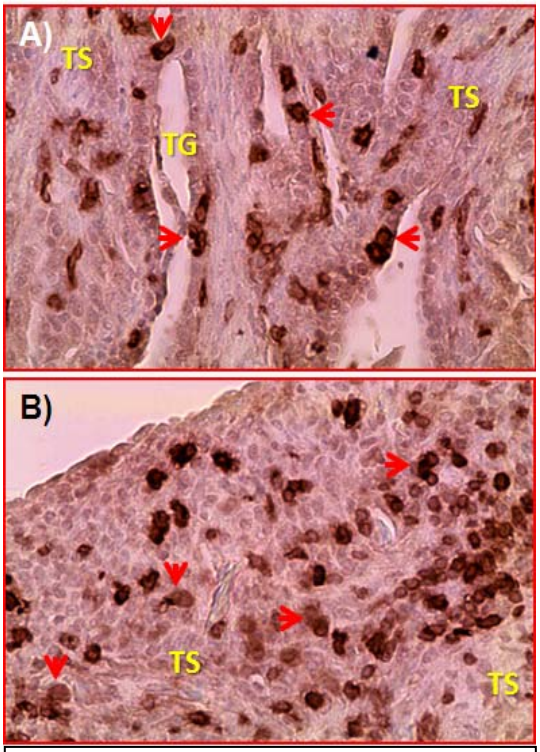

Figure 3. Changes in the population of IL-16 expressing cells in association with ovarian cancer (OVCA) development in hens. A) Section of a well-developed ovarian adenocarcinoma showing IL-16 expression by malignant epithelium and stromal cells. B) Section of a poorly differentiated ovarian adenocarcinoma showing many IL-16-expressig cells. TG=tumor gland, TS=tumor stroma, Red arrows are the examples of IL-expressing cells. 40X

Determination of serum IL-16 levels:

All serum samples collected during prospective scans were examined for IL-16 levels and changes in its level in association with OVCA development were examined. Serum levels of IL-16 were determined using Chicken IL-16 Vetset^{TM} ELISA Kit (Kingfisher Biotech, St. Paul, MN) pre-coated with anti-Chicken IL-

16 antibodies and chicken IL-16 as standards as per the manufacturer's instructions reported earlier and as reported previously [5]. Serum IL-16 levels in hens increased in association with ovarian tumor development. Significant increase in serum IL-16 levels was detected in hens with early stage OVCA which increased further in hens at late stages of OVCA.

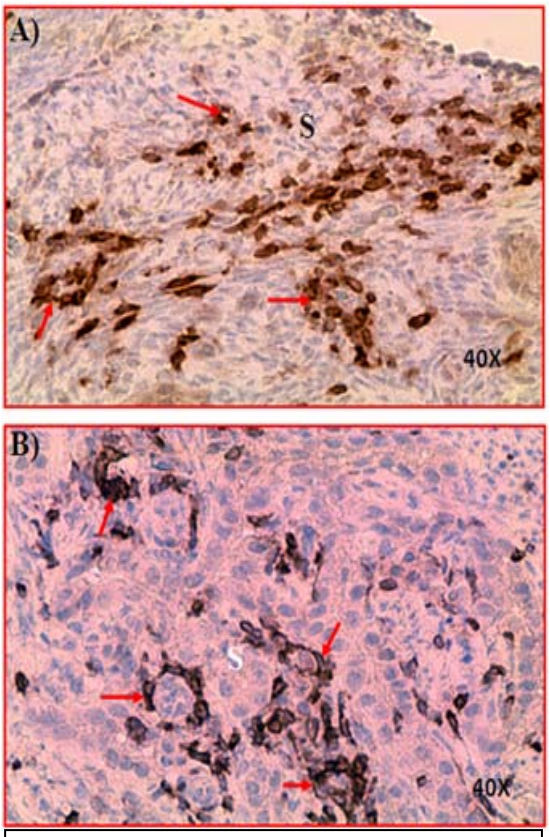

Figure 4: Ovarian tumor associated expression of IL-16 by microvessels in hens with OVCA detected by IL-16-targeted molecular ultrasound imaging. A) Section of an ovary with early stage OVCA. Endothelial cells of microvessels seen stained for IL-16. B) Section of late stage ovarian tumor. More microvessels are seen to express IL-16 in the tumor stroma (S). IL-16 expressing microvessels appeared leaky and surrounded by incomplete endothelial layer. Arrows indicate examples of IL-16 – expressing microvessels. 40X

Detection of IL-16 expression by ovarian tumors and ovarian tumor associated microvessels:

Tissue expression of IL-16 was examined immunohistochemically. Malignant cells in OVCA hens stained for IL-16 (**Figure 3A**). In ovaries with tumor at early stage, many stromal cells including immune cells were positive for IL-16 expression. Compared with well developed tumors, IL-16 expression by the tumor cells were remarkably high in poorly developed tumors (**Figure 3A-B**). The population of IL-16 expressing cells increased further in tumors at late stage. For the first time, this study has shown the expression of IL-16 by the endothelium of tumor associated microvessels (**Figure 4**). The population of IL-16 expressing microvessels increased as the tumor progressed to late stages.

Thus, as reported earlier, increased expression of IL-16 by malignant cells, stromal cells as well as endothelial cells of microvessels might be the reasons of increased serum IL-16 levels in hens associated with ovarian malignant development and progression. Moreover, increased tissue expression of IL-16 might also a reason of increased signal intensity of IL-16-targeted ultrasound imaging as compared with pre-targeted imaging.

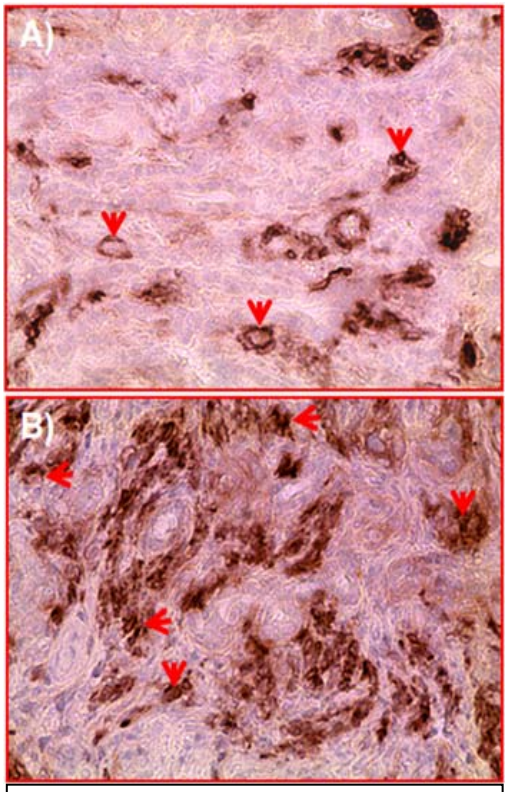

Figure 5. Changes in the expression of a-smooth muscle actin (α-SMA) by tumor associated microvessels in hen ovary during OVCA development. A) Tumor associated microvessels expressing α-SMA were localized in the stroma of a well-developed ovarian adenocarcinoma. B) Expression of α-SMA was intense in a poorly differentiated ovarian adenocarcinoma. Arrows are the examples of α-SMA expressing vessels in the stroma of ovarian tumors. 40X.

Detection of α-SMA expressing microvessels:
Tumor associated neo-angiogenesis is one of the earlier events in OVCA development and progression. The population of α-SMA-expressing microvessels was determined by immunhistochemistry as reported earlier [5]. The frequency of α-SMA-expressing microvessels increased remarkably in association with OVCA development and progression (**Figure 5**). Increased population of microvessels might be involved in increased blood flow to the growing tumor and thus are associated with lower RI and PI values in tumor hens as observed by the Doppler sonogram (**Figure 1E**).

***Detection of anti-NMP antibodies in serum of hens during prospective monitoring*:** Serum samples collected at different scan intervals were tested for the presence of anti-NMP antibodies using NMPs from archived ovarian tumor NMPs collected in Aim 1. Collection of NMPs and detection of anti-NMP antibodies by immunoassay were performed as reported earlier [4, 13, 12]. Briefly, 96-well ELISA plates (NUNC) were coated with tumor NMPs and the immunoreactivities of serum samples from each hen collected at different scanning intervals were tested against the coated tumor NMPs. Each serum sample was assayed in duplicate and the plates were read at 405nm in an ELISA plate reader (Softmax Pro, version 1.2.0, software; Molecular Devices, Sunnyvale, CA). Serum from normal hens with fully functional ovaries was used as negative control (established in earlier studies) for the presence of anti-NMP antibodies. Serum with optical density (OD) values higher than the control mean + 2SD (cut-off value) were considered positive for the presence of anti-NMP antibodies.

All hens positive for serum anti-NMP antibodies during initial scan remained positive throughout the prospective scanning completed so far. Hens with apparently normal ovaries are currently under monitoring. Representative serum samples with positive reactivity against tumor NMPs were analyzed by immunoproteomic study (2 dimensional-Western blotting, 2D-WB) to confirm immunoreactivities observed in ELISA. Immunoreactive NMPs of different sizes with a dense band at approx. 30-100kDa were detected by 2D-WB (**Figure 6**) confirming the results of ELISA for the prevalence of anti-NMP antibodies in serum.

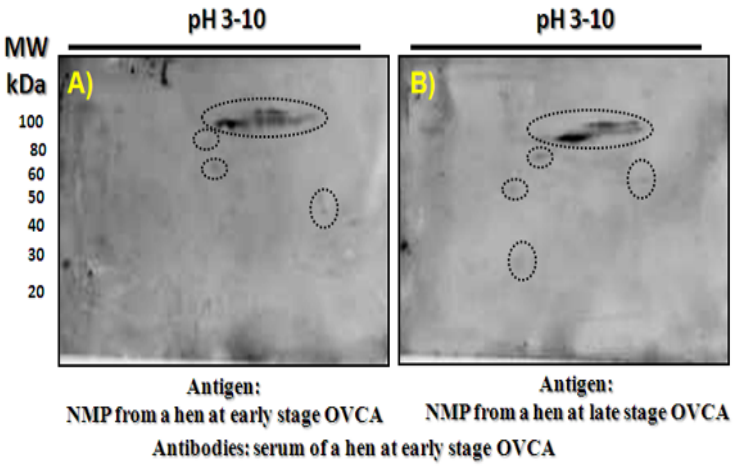

Figure 6. Detection of serum prevalence of anti-NMP antibodies in hens. Serum from a hen at early stage OVCA detected by IL-16-targeted molecular ultrasound imaging were examined against NMPs from heterogenous ovarian tumors A) at early stage and ***B***) at late stage. Nuclear matrix proteins (NMPs) were resolved and separated according to their molecular weight (MW) and pH and immunoblotted by 2dimensional Western blotting, 2D-WB. The same OVCA serum reacted in similar patterns against the NMPs from early and late stage OVCA. Serum from OVCA hens specifically detected ovarian NMPs of 30-100kDa. These results suggest that malignant nuclear transformation is associated with the prevalence of anti-NMP antibodies in serum.

KEY RESEARCH ACCOMPLISHMENTS IN YEAR 2 AND WORKS REMAINING TO BE COMPLETED:

- IL-16-targeted imaging agents bounded with their targets in ovary. The results so far obtained confirmed the observation of Aim-1 that IL-16-targeted imaging agents enhance ovarian tumor detection at early stage.
- Serum levels of IL-16 increase in relation to tumor associated enhanced tissue expression of IL-16.
- Malignant nuclear transformation (as indicated by the prevalence of anti-NMP antibodies in serum) and serum IL-16 levels may differentiate hens destined to develop OVCA later from non-OVCA hens.
- Expression of IL-16 by tumor associated microvessels is a noble finding of this study. Thus, IL-16-expressing microvessels can be targeted to inhibit tumor associated neoangiogenesis and OVCA progression.
- Determination of overall predictability of IL-16-targeted imaging agents in detecting early stage OVCA needs to allow the development of OVCA in most of the hens with serum anti-NMP antibodies group. Thus prospective monitoring of hens needs to be continued further for additional 12 weeks.
- One of the important information required for screening for OVCA is the time needed for hens with serum anti-NMP antibodies to develop a solid mass detectable by IL-16-targeted imaging. This time of incidence of solid mass in the ovary should be the median (incidence of OVCA in most of the hens) in weeks/months. This information will lead to the suitability of these markers for a screening protocol to detect early stage OVCA in clinical setting. Therefore, to determine the median time of first OVCA incidence detectable by the targeted imaging, the remaining hens with serum anti-NMP antibodies need to be monitored further for another 12 weeks.

REPORTABLE OUTCOMES DURING YEAR-2:

Presentation: Abstract published and presented:

1. ***Invited Oral presentation:*** Barua A, Yellapa A, Bitterman P, Bahr JM, Basu S, Sharma S and Abramowicz JS. *Contrast enhanced interleukin 16 targeted imaging detects ovarian tumor at early stage*. 10th Biennial **Ovarian Cancer Research Symposium**, September 8-9, 2014, Seattle, WA. (*Copy appended in appendix 1, pages 14-15*).
2. Yellapa A, Bahr JM, Grasso S, Sharma S and Barua A. *Interleukin-16 enhances ovarian tumor associated neoangiogenesis*. American Journal of Reproductive Immunology 71 (Suppl. 1) (2014) 35–36. 34th Annual Meeting of the **American Society for Reproductive Immunology**, 2–5 June, 2014, Long Beach, New York. *(Copy appended in appendix 2, pages 16-17)*

Manuscript:

Under review: Barua A, Yellapa A, Bahr J, Adur M, Bitterman P, Basu S, Sharma A and Abramowicz J. Interleukin 16 (IL-16)-targeted ultrasound imaging agent improves detection of ovarian tumors in laying hens, a preclinical model of spontaneous ovarian cancer. *BioMed Research International*. (Copy appended in appendix 3, pages 18-48)

Manuscript # 2 is under preparation.

CONCLUSIONS:

With the completion of Year 2, part of the results so far obtained suggest that compared with non-targeted traditional TVUS scanning, IL-16-targeted imaging agents enhanced ultrasound signals and improved the detection of ovarian tumors at early stage in hens. The enhancement of signal intensities by targeted imaging agents was due to their bindings with targets in the ovary. This enhancement in signal intensities was associated with increased expression of IL-16 by the ovarian malignant cells, stromal cells as well as by tumor associated microvessels. Serum levels of IL-16 increased in association with malignant transformation in the ovary. Similarly, results on anti-NMP antibodies confirmed that anti-NMP antibodies become prevalent before the tumor becomes detectable by ultrasound-imaging. With the completion of proposed extended monitoring period current results will be further confirmed and the feasibility of IL-16-targeted imaging agents and serum markers for the early detection of OVCA will be determined.

REFERENCES

[1] Siegel, R., D. Naishadham and A. Jemal (2012). "Cancer statistics, 2012." CA Cancer J Clin **62**(1): 10-29.
[2] Ries, L. A. (1993). "Ovarian cancer. Survival and treatment differences by age." Cancer **71**(2 Suppl): 524-9.
[3] Barua, A., Qureshi. T, Bitterman. P, Bahr. JM, Basu. S, Edassery. SL and Abramowicz. JS (2012). "Molecular targeted imaging of vascular endothelial growth factor receptor (VEGFR)-2 and anti-NMP autoantibodies detect ovarian tumor at early stage " In: Proceedings of the 103rd Annual Meeting of the American Association for Cancer Research; 2012 Mar 31-Apr 4; Chicago, IL. Philadelphia (PA): AACR; Cancer Res 2012; 72(8 Suppl): Abstract nr 2455. doi:1538-7445.AM2012-2455
[4] Yu, E., H. Lee, W. Oh, B. Yu, H. Moon and I. Lee (1999). "Morphological and biochemical analysis of anti-nuclear matrix protein antibodies in human sera." J Korean Med Sci **14**(1): 27-33.
[5] Yellapa, A., J. M. Bahr, P. Bitterman, J. S. Abramowicz, S. L. Edassery, K. Penumatsa, S. Basu, J. Rotmensch and A. Barua (2012). "Association of interleukin 16 with the development of ovarian tumor and tumor-associated neoangiogenesis in laying hen model of spontaneous ovarian cancer." Int J Gynecol Cancer **22**(2): 199-207.
[6] Moore, R. G. and R. C. Bast, Jr. (2007). "How do you distinguish a malignant pelvic mass from a benign pelvic mass? Imaging, biomarkers, or none of the above." J Clin Oncol **25**(27): 4159-61.
[7] Barua, A., J. S. Abramowicz, J. M. Bahr, P. Bitterman, A. Dirks, K. A. Holub, E. Sheiner, M. J. Bradaric, S. L. Edassery and J. L. Luborsky (2007). "Detection of ovarian tumors in chicken by sonography: a step toward early diagnosis in humans?" J Ultrasound Med **26**(7): 909-19.
[8] Anderson, C. R., J. J. Rychak, M. Backer, J. Backer, K. Ley and A. L. Klibanov (2010). "scVEGF microbubble ultrasound contrast agents: a novel probe for ultrasound molecular imaging of tumor angiogenesis." Invest Radiol **45**(10): 579-85.
[9] Barua, A., A. Yellapa, J. M. Bahr, S. A. Machado, P. Bitterman, S. Basu, S. Sharma and J. S. Abramowicz (2013). "Enhancement of Ovarian Tumor Detection With alphavbeta3 Integrin-Targeted Ultrasound Molecular Imaging Agent in Laying Hens: A Preclinical Model of Spontaneous Ovarian Cancer." Int J Gynecol Cancer.
[10] Barua, A., P. Bitterman, J. M. Bahr, M. J. Bradaric, D. B. Hales, J. L. Luborsky and J. S. Abramowicz (2010). "Detection of tumor-associated neoangiogenesis by Doppler ultrasonography during early-stage ovarian cancer in laying hens: a preclinical model of human spontaneous ovarian cancer." J Ultrasound Med **29**(2): 173-82.

[11] Barua, A., P. Bitterman, J. S. Abramowicz, A. L. Dirks, J. M. Bahr, D. B. Hales, M. J. Bradaric, S. L. Edassery, J. Rotmensch and J. L. Luborsky (2009). "Histopathology of ovarian tumors in laying hens: a preclinical model of human ovarian cancer." Int J Gynecol Cancer **19**(4): 531-9.
[12] Barua A, Qureshi T, Bitterman P, Bahr JM, Basu S, Edassery SL and Abramowicz JS (2012). "Molecular targeted imaging of vascular endothelial growth factor receptor (VEGFR)-2 and anti-NMP autoantibodies detect ovarian tumor at early stage." In: Proceedings of the 103rd Annual Meeting of the American Association for Cancer Research; 2012 Mar 31-Apr 4; Chicago, IL. Philadelphia (PA): AACR; Cancer Res 2012; 72(8 Suppl): Abstract nr 2455. Doi:1538-7445.AM2012-2455
[13] Barua, A., S. L. Edassery, P. Bitterman, J. S. Abramowicz, A. L. Dirks, J. M. Bahr, D. B. Hales, M. J. Bradaric and J. L. Luborsky (2009). "Prevalence of antitumor antibodies in laying hen model of human ovarian cancer." Int J Gynecol Cancer **19**(4): 500-7.
[14] Anderson, C. R., X. Hu, H. Zhang, J. Tlaxca, A. E. Decleves, R. Houghtaling, K. Sharma, M. Lawrence, K. W. Ferrara and J. J. Rychak "Ultrasound molecular imaging of tumor angiogenesis with an integrin targeted microbubble contrast agent." Invest Radiol **46**(4): 215-24.
[15] Bradaric, M. J., A. Barua, K. Penumatsa, Y. Yi, S. L. Edassery, S. Sharma, J. S. Abramowicz, J. M. Bahr and J. L. Luborsky (2011). "Sphingosine-1 phosphate receptor (S1p1), a critical receptor controlling human lymphocyte trafficking, is expressed in hen and human ovaries and ovarian tumors." J Ovarian Res **4**(1): 4.
[16] Barua, A. and Y. Yoshimura (1999). "Effects of aging and sex steroids on the localization of T cell subsets in the ovary of chicken, Gallus domesticus." Gen Comp Endocrinol **114**(1): 28-35.
[17] Hong, Y. H., H. S. Lillehoj, S. H. Lee, R. A. Dalloul and E. P. Lillehoj (2006). "Analysis of chicken cytokine and chemokine gene expression following Eimeria acervulina and Eimeria tenella infections." Vet Immunol Immunopathol **114**(3-4): 209-23.

The Marsha Rivkin Center for Ovarian Cancer Research

Animesh Barua PhD
Rush University Medical Center
Cohn Building, Room#410
1735 W. Harrison St
Chicago, IL 60612

17 June 2014

Dear Dr. Barua,

The Planning Committee for the 10th Biennial Ovarian Cancer Research Symposium has conducted a thorough review of nearly 190 submitted abstracts. We are pleased to notify you that your abstract entitled "Contrast enhanced interleukin 16 targeted imaging detects ovarian tumor at early stage" has been selected for oral presentation in the scientific session "Strategies for Controlling Ovarian Cancer". The Symposium will take place on Monday and Tuesday, September 8-9, 2014 in Seattle, Washington.

If you would like to accept our invitation, please complete and return the attached forms to me via email by Monday, June 30th, 2014. The Symposium is an accredited activity by the Accreditation Council for Continuing Medical Education (ACCME), and all speakers must provide the requested information. Also contained in the attached PDF are details concerning your participation including the deadline for submitting your presentation as well as the travel stipend being offered to you, which is intended to help defray costs, but may not entirely cover your expenses.

It is our pleasure to waive the Symposium registration fee. You do not need to register yourself online as we will automatically register you if you accept our invitation.

If you have any questions, please contact me at (206) 215-2964 or Wendy.Law@swedish.org. On behalf of the Rivkin Center, Swedish Medical Center, and the American Association for Cancer Research, we would like to express our enthusiasm about your research and hope to see you in Seattle this September!

Best Wishes,

Wendy Law, PhD
Director of Scientific Programs

ATTACHMENT

Contrast enhanced interleukin 16 targeted imaging detects ovarian tumor at early stage

Animesh Barua[1], Aparna Yellapa[1], Pincas Bitterman[1], Janice M Bahr[2], Sanjib Basu[1], Sameer Sharma[1] and Jacques S. Abramowicz[1,3]

[1]Rush University Medical Center, Chicago and [2]University of Illinois at Urbana-Champaign, IL, [3]Wayne State University, Detroit, MI

Background: The high rate of death of ovarian cancer (OVCA) patients can be reduced if it is detected at early stage. Neither suggested serum markers nor the currently available traditional transvaginal ultrasound (TVUS) imaging or their combinations can detect OVCA at early stage. No imaging target in the ovary for TVUS imaging corresponding to the suggested serum markers has been defined. Moreover, due to the limited resolution, TVUS imaging cannot detect OVCA at early stage. Thus, new imaging target(s) together with improvement in resolution is necessary for early OVCA detection by TVUS imaging. Interleukin 16 (IL-16), a proinflammatory cytokine, associated with longstanding unresolved inflammation due to frequent ovulation, has been reported to be increased during OVCA development. IL-16 is expressed by the ovarian malignant cells and tumor associated neoangiogenic (TAN) microvessels. Thus IL-16 represents a potential marker of early OVCA which can be detected *in vivo* by TVUS imaging provided a molecular targeted contrast enhanced imaging agent can be developed.

Objective: The goal of this study was to develop and test the efficacy of molecular (IL-16)-targeted ultrasound imaging probe for the detection of early OVCA.

Materials and Methods: 3-years old (n=150) White Leghorn laying hens with normal or low egg laying rates or stopped-egg laying were scanned by TVUS before and after intravenous injection with IL-16-targeted microbubbles. IL-16-targeted imaging agents were prepared by conjugating anti-chicken IL-16 antibodies with Targetster ® containing microbubbles (Targeson Inc, San Diego). All images were archived and analyzed offline. Serum samples were collected, hens were euthanized, ovarian tissues were processed for paraffin or frozen sections and nuclear matrix protein (NMP) extraction. Ovarian tumors were confirmed by gross morphology and routine histology. Sera were tested for anti-NMP antibodies (a marker of malignant nuclear transformation) and IL-16 levels by immunoassay and 1- & 2D-Western blot (WB). The frequencies of IL-16 expressing cells were determined by immunohistochemistry (IHC).

Results: IL-16-targeted microbubbles bounded with ovarian tumors and appeared as shining mass of irregular-shape. Compared with non-targeted, IL-16-targeted imaging increased the visualization of ovarian tumors remarkably. All hens with suspected tumor mass (n=23, 7 early and 16 late stages) were detected by IL-16-targeted imaging and confirmed by gross examination. The frequency of IL-16 expressing cells detected by IHC confirmed the prediction of targeted ultrasound imaging. Serum levels of IL-16 were higher in OVCA hens than in normal hens and correlated with the frequencies of IL-16 expressing cells and ovarian TAN vessels. Prevalence of anti-NMP antibodies were not detected in normal hens while all hens with OVCA were positive. Immunoreactive tumor antigens (NMPs) of 50-80kDa were detected by 2D-WB.

Conclusion: IL-16-targeted ultrasound imaging enhanced the visualization of ovarian tumors remarkably. The enhanced intensity of IL-16-targeted imaging was correlated with serum IL-16 levels and the prevalence of anti-NMP antibodies. Thus, IL-16-targeted imaging in association with serum anti-NMP antibodies may improve OVCA detection at early stage. These results will form a foundation for a clinical study. *Support*: Dept. of Defense award # W81XWH-12-1-0460.

tation protection against environmental toxins. In parallel, PIF enhances trophoblast invasion balancing TIMP/integrin ratio as well up-regulating trophoblastic pro-tolerance HLA-G expression. Finally, *in vivo* PIF administration maximizes the number of implantation sites that successfully reach the fetal stage (murine). Collective data corroborates that PIF-initiated maternal recognition orchestrates maternal adaptation that is required for successful pregnancy outcome.
*PIF Proprietary

G-12

IL-33-responsive group 2 innate lymphoid cells are present in mouse uterine tissue and may play roles in healthy pregnancy

KR Bartemes[1], H Kita[2]
[1]Department of Immunology, Mayo Clinic, MN, USA; [2]Department of Medicine, Mayo Clinic, MN, USA

Problem: Group 2 innate lymphoid cells (ILC2s) that are responsive to IL-33 drive helminth immunity, type 2 immune responses, and tissue pathology and homeostasis in mucosal organs, such as lungs and skin. Considering their biological effects, ILC2s may also play a role in the placenta and be involved in fetus-protective type 2 immunity. Indeed, recent reports have implicated changes in levels of both IL-33 and soluble IL-33 receptor (i.e. sST2) in spontaneous abortion and pre-eclampsia. Here, we sought to examine the presence of ILC2s in uterine tissue and investigate the effects of ST2 deficiency on successful pregnancy outcomes in mice.
Methods of study: Single cell suspensions of murine uteri were examined by flow cytometry for the presence of ILC2s. Dynamic changes in ILC2s in uteri were examined in IL-5-reporter mice by administering IL-33 systemically. To examine the role of IL-33/ST2 signaling in healthy pregnancy, ST2−/− females (on a Balb/c background) were mated with ST2−/−, MHC-matched Balb/c and MHC-mismatched C57B6 males. Balb/c, C57B6 and Balb/c × C57B6 pairs were used as controls. Litter sizes and numbers of non-viable pups (survival less than 24 hr) were examined.
Results: Lineage-negative, CD25+ and CD44+ ILC2s were found in normal murine uteri. Systemic administration of IL-33 to naïve Balb/c mice increased the ILC2 numbers in uteri and induced IL-5 production by them *in vivo*, suggesting that IL-33 affects the number and activity of uterine ILC2s. Litter sizes were not significantly different among the pairings irrespectively of their genotypes. However, total numbers of non-viable pups, percent of litters with at least one non-viable pup and percent of non-viable pups per litter were significantly increased in ST2−/− × C57B6 pairs when compared to control pairs.
Conclusion: IL-33-responsive ILC2s are present in murine uterine tissue and may play pivotal roles in successful reproduction.

G-13

Interleukin-16 enhances ovarian tumor associated neoangiogenesis

A Yellapa, JM Bahr, S Grasso, S Sharma, A Barua
Rush University Medical Center, Chicago University of Illinois at Urbana-Champaign, IL, USA

Problems: Ovarian cancer (OVCA), a lethal malignancy of women, disseminates locally in the peritoneal cavity. Tumor microenvironment plays important roles in OVCA metastasis. Tumor associated neo-angiogenesis (TAN) is a hall mark of OVCA progression and cytokines may stimulate the establishment of early TAN. Interleukin (IL)-16, a pro-inflammatory cytokine is associated with OVCA development. The goal of this study was to examine whether IL-16 stimulates ovarian TAN during OVCA development.
Method of study: Four years old White Leghorn laying hens with (n = 17) or without (n = 20) ovarian tumors were selected by ultrasound scanning and OVCA stages was determined following euthanasia. Ovarian tissues and serum samples from hens were processed for immunoassay, immunohistochemistry (IHC), proteomic and gene expression studies for IL-16 and SMA-expressing micro vessels. Normal ovarian epithelial cells were treated with IL-16 to determine expression of IL-8, an angiogenic factor. HUVEC cells were examined for CD9 (receptor for IL-16) expression. Differences in IL-16 expression and micro vessel frequencies among normal and OVCA hens were determined by one-way ANOVA and paired T-tests.
Results: OVCA were limited to the ovaries in eight hens (early stage) and metastasized in nine hens (late stage). IL-16 expression was significantly

($P < 0.01$) high in hens with early stage OVCA and increased further in late stage OVCA. Frequency of SMA-expressing micro vessels were significantly ($P < 0.001$) high in OVCA hens than normal hens. Increase in IL-16 expression in OVCA hens was positively correlated with the frequencies of SMA-expressing micro vessels. A strong band for IL-8 was detected in IL-16 treated cells and HUVAC cells expressed CD9 proteins.

Conclusion: The results suggest that changes in IL-16 expression were associated with increased frequency of SMA-expressing micro vessels. IL-16 enhanced expression of IL-8, possibly through its receptor CD9. These results suggest a novel role of IL-16 and may be useful in designing antitumor immune therapeutics targeting IL-16 for OVCA prevention.

Support: DOD ovarian cancer pilot award # W81XWH-12-1-0460.

G-14

Chorioamnionitis induced by inactivated group B streptococcus: from placental lesions to autism spectrum disorders features

JD Bergeron[1], ME Brochu[1], C Guiraut[1], LC Fortier[2], C Poyart[3], G Sébire[1]

[1]Department of pediatrics, Université de Sherbrooke & McGill University, Canada; [2]Department of microbiology, Université de Sherbrooke, Canada; [3]Institut Cochin, Université de Paris, France

Problem: A high incidence of neurobehavioral disorders, such as autism spectrum disorders, occurs in children born to mothers who experienced infections during pregnancy. According to our hypothesis group B streptococcus (GBS) induced maternal immune activation plays a role in placental lesions and offspring subsequent neurobehavioral disabilities.

Methods of study: We designed a new pre-clinical animal model in which dams were injected every 12 hr with inactivated GBS (109 CFU) from serotype 1a GBS, versus saline, from gestational day (G) 19 to G22. Some dams gave birth naturally at G23 (behavioral studies with pups) and C-sections were performed at G22 on other dams to remove placentas for immunohistochemical studies and proteins analysis.

Results: GBS-exposed placentas presented cystic lesions and polymorphonuclear infiltration located within the decidual/maternal side of the placenta. Interestingly, preliminary results showed higher level of PMN infiltration and expression of MMP8 in placentas associated with male than those associated with female fetuses. Surprisingly, cardinal features of human autism were found predominantly in males, characterized mainly by social interactions impairments, lack of exploratory behavior and singular sensory processing.

Conclusions: Our results show for the first time that materno-fetal inflammatory response to GBS plays a role in the induction of placental insults and neurobehavioral disabilities in offspring. Placental lesions and changes in placental proteins may spread through a fetal inflammatory reaction syndrome (FIRS) affecting developmental processes of the offspring's brain, thereby increasing its susceptibility to ASD, especially for males.

G-15

Distinct microRNA and their putative target mRNA expression in endometrial lymphocytes, endometrium and trophoblast during healthy and abortive porcine pregnancy

M Bidarimath[1], AK Edwards[1], JM Wessels[2], K Khalaj[1,2], RT Kridli[2,3], C Tayade[1,2]

[1]Department of Biomedical and Molecular Sciences, Queen's University, Kingston, ON, Canada; [2]Department of Biomedical Sciences, Ontario Veterinary College, University of Guelph, Guelph, Ontario, Canada; [3]Department of Animal Production, Faculty of Agriculture, Jordan University of Science and Technology, Irbid, Jordan

Problem: Approximately 25–40% genetically normal conceptuses are spontaneously lost during peri-attachment and mid-pregnancy in pigs. A deficit in vasculature is one of the major factors associated with conceptus loss. During early pregnancy, endometrial lymphocytes are uniquely recruited to the maternal-fetal interface by conceptus derived signals. They adopt a specialized phenotype that regulates placental angiogenesis but precise mechanism is not known. microRNAs are emerging as bio-regulatory molecules of various processes including angiogenesis. We hypothesize that microRNAs are involved in development of endometrial lymphocytes and their angiogenic functions at the maternal-fetal interface.

Methods of study: Laser capture micro dissected endometrial lymphocytes, endometrium, and trophoblasts associated with healthy and spontaneously

Hindawi Publishing Corporation

Hindawi

Animesh Barua Update My Account Logout

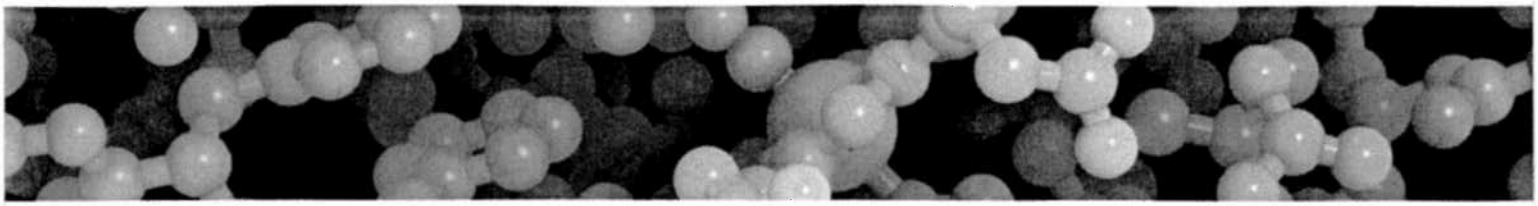

Submit a Manuscript Author Activities

567459.v1 (Research Article)

Title	Interleukin 16 (IL-16)-targeted ultrasound imaging agent improves detection of ovarian tumors in laying hens, a preclinical model of spontaneous ovarian cancer
Journal	BioMed Research International
Subject Area	Obstetrics and Gynecology
Issue	Challenges in Gynecological Cancer: Biology, Diagnosis, Surgical, and Medical Treatment (CGC)
Additional Files	Cover Letter
Manuscript Number	567459 (Research Article)
Submitted On	2014-09-21
Author(s)	**Animesh Barua**, Aparna Yellapa, Janice Bahr, Malavika Adur, Pincas Bitterman, Sanjib Basu, Sameer Sharma, Jacques Abramowicz
Editor	Elisa Piovano
Status	Under Review

Interleukin 16 (IL-16)-targeted ultrasound imaging agent improves detection of ovarian tumors in laying hens, a preclinical model of spontaneous ovarian cancer

Animesh Barua[1, 2, 3], Aparna Yellapa[1], Janice M Bahr[4], Malavika K Adur[4], Pincas Bitterman[2, 3], Sanjib Basu[5], Sameer Sharma[1, 2] and Jacques S Abramowicz[2, 5]

Departments of [1]Pharmacology, [2]Obstetrics and Gynecology, [3]Pathology, [5]Preventive Medicine (Biostatistics), Rush University Medical Center; [4]Department of Animal Sciences, University of Illinois at Urbana-Champaign, Illinois; [5]Department of Obstetrics and Gynecology, Wayne State University, Detroit, MI

Short Title: IL-16- targeted imaging of ovarian tumors

Correspondence to:
Animesh Barua, Ph.D.
Laboratory for Translational Research on Ovarian Cancer,
Department of Pharmacology
Room # 410, Cohn Building,
Rush University Medical Center
1735 W. Harrison St., Chicago IL 60612
Tel. 312-942-6666
Fax: 312-563-3552
Animesh_Barua@rush.edu

Abstract

Limited resolution of transvaginal ultrasound (TVUS) scanning is a significant barrier to early detection of ovarian cancer (OVCA). Contrast agents have been suggested to improve the resolution of TVUS scanning. Emerging evidence suggests that expression of interleukin 16 (IL-16) by the tumor epithelium and microvessels increase in association with OVCA development and offers a potential target for early OVCA detection. The goal of this study was to examine the feasibility of IL-16-targeted contrast agents in enhancing the intensity of ultrasound imaging from ovarian tumors in hens, a model of spontaneous OVCA. Contrast agents were developed by conjugating biotinylated anti-IL-16 antibodies with streptavidin coated microbubbles. Enhancement of ultrasound signal intensity was determined pre-and-post-injection of contrast agents. Following scanning, ovarian tissues were processed for the detection of IL-16-expressing cells and microvessels. Compared with pre-contrast, contrast imaging enhanced ultrasound signal intensity significantly in OVCA hens at early (P <0.05) and late stages (P <0.001). Higher intensities of ultrasound signals in OVCA hens were associated with increased frequencies of IL-16-expressing cells and microvessels. These results suggest that IL-16-targeted contrast agents improve the visualization of ovarian tumors. The laying hen may be a suitable model to test new imaging agents and develop targeted anti-OVCA therapeutics.

1. Introduction

The global yearly rate of death of women due to ovarian cancer (OVCA) is approximately 140, 200 women and that of the USA is approximately 15,000[1, 2] making OVCA one of the lethal gynecological malignancies. Because of the lack of an effective early detection test, OVCA in most cases is detected at late stages. Development of resistance to currently available chemotherapeutics and frequent recurrences when detected at late stages decrease 5-year survival rate of OVCA patients to <20%. In contrast, OVCA can be cured in >90% cases when it is detected at early stage. Therefore, early detection of OVCA is crucial and an effective early detection test is urgently needed. Serum levels of CA-125 alone or in combination with traditional transvaginal ultrasound (TVUS) imaging is the currently available test for the detection of OVCA [3]. However, neither the CA-125 nor the TVUS can detect OVCA at early stage specifically as serum CA-125 level is elevated in patients with several benign gynecological as well as non-gynecological abnormalities. On the other hand, although TVUS is the currently available preferred method for non-invasive imaging of ovarian abnormalities, unfortunately, with its limited resolution, traditional TVUS cannot detect OVCA at early stage [4]. In addition, a combination of serum CA-125 levels together with traditional TVUS imaging also failed to detect early OVCA as no imaging target in the ovary corresponding to the elevated serum CA-125 levels is established [4]. Thus a fresh approach is needed.

Extensive studies have been performed on the establishment of serum biomarkers for the detection of OVCA at early stage and a plethora of serum based marker(s) have been suggested. However, due to their lack of specificity and sensitivity, none of these markers was successful in detecting OVCA at early stage indicating that serum marker(s) alone may not be able to detect OVCA at early stage. Thus, an imaging target related to the malignant transformation of the

ovary needs to be established and the current detection limit of traditional TVUS needs to be enhanced to detect early OVCA-related changes in the ovary. Moreover, to facilitate early detection of OVCA specifically, this imaging target(s) should also be associated with a surrogate maker(s) to be detectable in the serum. Contrast agents have been developed to enhance the visualization of tumors by several imaging modalities including TVUS scanning [5-9]. Imaging agents targeting αvβ3-integrins and vascular endothelial growth factor receptor 2 (VEGFR2) have been developed for contrast enhanced ultrasound imaging [10, 11]. However, very few reports are available on the ability of these targeted contrast agents in detecting OVCA at early stage. Moreover, absence of a corresponding serum surrogate marker reduces the specificity and sensitivity of these imaging agents. Thus additional imaging target(s) associated with malignant transformation needs to be established and imaging agents needs to be developed to detect these new imaging targets for early detection of OVCA with high specificity.

Inflammation has been suggested as a risk factor for malignant transformation [12]. Unresolved inflammation leads to hypoxic conditions accompanied by changes in inflammatory cytokines including interleukin (IL)-16 [12, 13]. Ovulation is an inflammatory process which exposes ovarian surface (at the site of ovulatory rupture) and fimbrial epithelium (the site of reception of the ovulated ovum) to inflammatory factors including IL-16 secreted by immune cells. Exposure of the ovary and tubal epithelium to inflammatory agents due to frequent ovulation leads to the development of oxidative stress and longstanding unresolved oxidative stress has been suggested to cause malignant transformation. On the other hand, expression of IL-16 by the tumor epithelium and its serum levels has been reported to increase in association with ovarian tumor development [14, 15]. Moreover, IL-16 has also been reported as a pro-angiogenic factor [16] and may also be expressed by the endothelium of tumor associated

microvessels. Thus IL-16 represents a potential marker of early OVCA and IL-16 expressing tissues in the ovary can be detected by ultrasound imaging provided an IL-16-targeted ultrasound imaging agent can be developed.

Identification and access to patients with early stage OVCA are the significant barriers to develop and test the efficacy of contrast enhancing imaging agents in detecting spontaneous OVCA at early stage. Most of the available contrast agents were developed using rodents, thus, are difficult to translate in human OVCA [17, 18, 11, 19]. Because, rodents do not develop OVCA spontaneously and induced ovarian carcinoma in rodents are histopathologically not similar to those of spontaneous OVCA in humans[20]. Recently, laying hens have been shown to develop OVCA spontaneously with high incidence rates. Spontaneous OVCA in hens are remarkably similar to human OVCA with regard to tumor histopathology and expression of several molecular markers [21, 20, 22-26, 14]. Furthermore, methods for the imaging of hen ovaries and ovarian tumors by TVUS scanning have been adapted [27-29]. Moreover, similar to humans, expression of IL-16 by ovarian tumors has been reported to be increased in association with tumor development and progression in hens, [14, 15]. Thus the laying hen represents a highly innovative model to test the feasibility of IL-16-targeted imaging agents for the detection of spontaneous OVCA at an early stage by non-invasive TVUS imaging. Therefore, the goal of this study was to examine whether IL-16-targeted contrast agents enhance the intensity of traditional TVUS imaging and improve the early detection of spontaneous ovarian tumors in laying hens, a preclinical model of OVCA.

2. Materials and Methods

2.1. Animals. A flock of 3-4-years old commercial strains of White Leghorn laying hens (*Gallus domesticus*) were maintained under standard poultry care and management and provided with feed and water *ad libitum*. Egg-laying rates of the hens were recorded on a daily basis. Egg laying rates in a hen is used as a relative indicator of ovulation rates in hens. The normal rate of egg laying by a commercial laying hen is more than 250 eggs per year, and less than 50% of the normal laying rate is considered a low egg-laying rate [27]. 150 hens with normal, low or irregular egg-laying rates and those that stopped laying with no large preovulatory follicle, with or without solid mass in the ovary and abdominal distention (a sign of possible ovarian tumor-associated ascites) were selected for IL-16-targeted contrast enhanced imaging agents. The incidence of ovarian cancer in laying hens of this age group was reported to be approximately 10% to 20% and is associated with low laying rates or complete cessation of egg laying [27, 21, 20]. All procedures were performed according to Institutional Animal Care and Use Committee approved protocol.

2.2. IL-16- targeted contrast enhanced ultrasound imaging agents. IL-16-targeted imaging agents were prepared by conjugating anti-chicken IL-16 antibodies with Targestar ® containing microbubbles (Targeson, Inc San Diego**,** CA). Targestar SA is a targetable ultrasound contrast agent coated with streptavidin. Biotinylated antibodies can be easily conjugated to the microsphere surface, enabling target-specific retention for molecular imaging. The agent remains acoustically active upto15 minutes. Agents are administered as an intravenous bolus injection. Microbubbles preparation, ligand conjugation, characterization of labeled microbubbles and their binding specificity of tumor tissues were similar to those reported earlier [10].

2.3. Ultrasound imaging

2.3.1. Pre-contrast traditional transvaginal ultrasound (TVUS) imaging. All hens were scanned using an instrument equipped with a 1 to 7.5-MHz transvaginal transducer (MicroMaxx; SonoSite, Inc, Bothell, WA) as reported previously with little modification [27, 29]. Hens were immobilized and gently restrained by an assistant. Transmission gel was applied to the surface of the transducer, the transducer was covered by a cover and to ensure uninterrupted conductance of the sound waves, gel was reapplied to the covered probe. The transducer was inserted approximately at a 30° angle to the body, 3 to 5 cm into the vagina and 2-dimensional (2D) gray scale and pulsed Doppler sonography were performed. Young egg-laying hens (as the ovaries of these hens contain more developing follicles compared to old hens) were used as standard controls for mechanical adjustment to reveal and characterize the fully functional normal ovaries of hens. The area of a tumor to be imaged was determined according to 3 conditions as reported previously [27, 29]: (a) the whole tumor, if possible, should be seen on the image; (b) the sectional plane should contain the solid part (wall, septa, and papillae) of the tumor; and (c) the most vascularized area was selected. For normal ovaries, ovaries without any detectable tumor, and atrophic ovaries, the region surrounding the ovary was scanned, and the transducer was swept through the entire area for complete scanning of the ovary. Gray scale morphologic evaluation of the ovarian mass was performed with attention to the number of preovulatory follicles, the presence of abnormal-looking follicles, septations, papillary projections or solid areas, and echogenicity. After morphologic evaluation, color Doppler mode was activated for identification of vascular color signals. Once a vessel was identified on color Doppler imaging, pulsed Doppler was activated to obtain a flow velocity waveform.

2.3.2. Injection of IL-16-targeted contrast agents and contrast enhanced ultrasound imaging. Contrast imaging was performed following pre-contrast scanning. A preliminary experiment was conducted with IL-16-targeted or isotype control microbubbles using 10 animals containing fully functional ovaries to adjust the mechanical setup and determine the optimum dosage of microbubbles. The dose of 10 µL/kg body weight was found optimal for better resolution in the preliminary experiment. Microbubbles containing contrast agents were prepared before injection. Briefly, the vial containing the microbubble suspension was inverted and gently rotated to re-suspend the microspheres completely. The suspension was transferred from the vial by an injection syringe with a 19-gauge needle to a angiocatheter (small-vein infusion set, female luer, 12-in tubing, 25-gauge needle; Kawasumi Laboratories, Tampa, FL) containing 100 µL of 0.9% sodium chloride previously inserted into the left wing vein (brachial vein) of the hen and followed by the reloading of 100 µL of a 0.9% sodium chloride solution. The loading of the sodium chloride solution before and after injection of microbubbles helped maintain the vascular patency and airtight condition, in addition to flushing the bubbles from the hen's circulation.

The area imaged during pre-contrast scanning was imaged again after contrast microbubble injection. Following injection of contrast agents and before post-contrast imaging, time was allowed for microbubbles to bind with their targets and retention of bounded microbubbles in the tumor as well as washing-out of unbound microbubbles. The timing of contrast imaging was determined through an initial experiment using different time points including 2, 5, 7 and 10min. Imaging after 7min of contrast agent injection was found optimum with minimum background signals. Then a destructive pulse was delivered and images were taken again. The difference in the intensity of ultrasound imaging between the images at 7min after injection and images after the delivery of destructive pulse confirms that the signal acquired

after contrast agent injection was from microbubbles-bounded target tissue. For an individual hen, the same imaging plane and same size of ROI was used for measuring the pre-contrast and post-contrast intensity of ultrasound imaging. All images (screen shots) were archived digitally in a still format as well as real-time clips on single-sided recordable digital video disks (DVD+R format; Maxell Corporation of America, Fair Lawn, NJ) readable on a personal computer.

2.3.3. Evaluation of the Effects of IL-16-Targeted Contrast Agents. The effect of contrast agents was evaluated visually during the examination and the enhancement of tumor detection by contrast imaging was assessed afterward from reviewing the archived video clips. After review of the complete clip the image containing the stroma of normal hens or containing the tumor were selected and used as region of interest (ROI) for measuring the pre-contrast and post-contrast intensity of ultrasound imaging. In normal hens, areas containing large developing follicles were avoided during the selection of images containing the ROIs. The intensity of the pixels in the selected area was measured using a computer-assisted software program (MicroSuite version 5; Olympus Corporation, Tokyo, Japan) and expressed as arbitrary values. The intensity of the ROI (sum of the arbitrary values from the pixels within the region of interest) was measured from the pre-contrast and contrast image and expressed as the mean $\pm$ SD in 40,000 pixel area. The net contrast enhancement (CE = Ct-Cpt) was determined and the CE ratio (CER) was calculated using the following equation: CER = (Ct-Cpt)/Cpt X 100% where Cpt = values from ROI of pre-contrast image and Ct = values from ROI of contrast image. As mentioned above, Ct is the difference between the intensity of ultrasound imaging from images taken at 7min after injection of contrast agents and after the delivery of a destructive pulse.

2.4. Ovarian gross morphologic evaluation. All hens were euthanized after contrast imaging and examined for the presence of a solid mass in the ovary as well as in any other organs, ascitic fluid, preovulatory follicles, and atrophy of the ovary, as reported previously[21]. Gross observation was compared with the sonographic evaluations and photographed. A normally functional ovary had viable preovulatory follicles (more detailed information on hen ovarian physiology has been published elsewhere [27, 21]), whereas no large follicles or visible lesions were found in normal hens that stopped egg laying. Tumor staging was performed according to the gross metastatic status as reported previously [21]. Briefly, early OVCA was characterized by detectable formation of solid tumor limited to the ovary. Late stages of OVCA were characterized by tumor metastasis to distant organs with moderate to extensive ascites.

2.5. Histologic evaluation and immunohistochemical detection of ovarian IL-16-expressing cells and microvessels. Representative portions of a solid ovarian mass or the whole ovary (in cases of atrophic or grossly normal-appearing ovaries) were divided into several blocks, processed for paraffin or frozen sections, and stained with hematoxylin-eosin. Microscopic tumor (if present) in any part of the ovary was detected by routine histologic examination with hematoxylin-eosin staining, and tumor types were determined by light microscopy, as reported previously [21].

After histopathologic examination, paraffin sections (5 μm thick) of normal and malignant ovaries of all stages and types were processed for routine immunohistochemistry to assess the frequency of IL-16-expressing cells and microvessels using rabbit anti-chicken IL-16 polyclonal antibodies as reported earlier [14, 15]. The frequencies of IL-16-expressing cells and microvessels were determined from the stroma of the ovarian tumors or ovarian stroma of

normal hens (excluding the follicular areas), as reported earlier [28, 30] using a light microscope attached to digital imaging stereological software (MicroSuite version 5; Olympus Corporation) with little modification. Briefly, immunostained slides were examined at low-power magnification (x10 objective and x10 ocular) to identify the areas with maximum IL-16-expressing cells or microvessels. Vessels with thick, regular, and complete muscular walls as well as vessels with large lumina were excluded from the count, as reported previously[28]. In each section, the 5 highly immunostained areas for IL-16 expressing cells or microvessels were chosen and immunopositive cells or microvessels (with leaky, incomplete and thin vessel wall) were counted. The number of immunopositive cells or microvessels in a 20,000-μm^2 area was counted at an x40 objective and x10 ocular magnification. The averages of these sections were expressed as the number of immunopositive cells or microvessels in a 20,000-μm^2 area of a normal ovary or ovary with tumor. Tumor histology and immunohistochemical observations were compared to the sonographic predictions.

2.6. Statistical Analysis. Descriptive statistics for imaging parameters were determined, and statistical analysis was performed in SPSS version 15 (SPSS Inc, Chicago, IL). The differences in the net intensities of ultrasound imaging and the frequencies of IL-16-expressing cells and microvessels among normal hens or hens with early and late stage OVCA were analyzed by the two-sample *t* test. The association between the intensity of ultrasound imaging and the frequency IL-16-expressing cells or microvessels was examined by Pearson coefficient of correlations. $P < 0.05$ was considered significant. All reported *P* values are 2 sided.

3. Results

3.1. Evaluation of non-invasive contrast enhanced ultrasound imaging. In normal hens with functional ovaries, multiple preovulatory follicles and small growing stromal follicles were observed on pre-contrast and contrast imaging. Compared to pre-contrast ovaries, visualization of solid ovarian masses with or without projected septa and papillary structures, accompanying ascites, or both were enhanced remarkably in the ovaries of 23 hens. Of these 23 hens, 16 had solid masses in the ovary together with profuse ascites and were predicted to have late-stage OVCA (**Figure 1A-B and C-D**). In the remaining 7 hens, solid masses were limited to a part of the ovary with no or little ascites, and they were provisionally categorized as early-stage OVCA (**Figures 2A and B**). Compared with pre-contrast scanning, IL-16-targeted contrast enhanced imaging improved the visualization of ovarian tumor masses in these 23 hens on gray scale (**Figures 1 and 2**). All of these hens were categorized as "hens with suspected ovarian cancer".

All hens were euthanized following IL-16-targeted contrast imaging and sonographic predictions as well as stages of the tumor were confirmed by gross examination of hens at necropsy (**Figures 1E and 2D**). Ovarian morphology including ovarian follicles and their sizes, oviducts, presence of solid mass in the ovary, levels of tumor metastasis, OVCA stages and accompanying ascites, were recorded and tissues were processed as mentioned above. Tumor types were determined by routine hematoxylin & eosin staining (H&E) of paraffin sections (**Figure 1F**). Staging of ovarian tumors was performed as reported previously [21]. As observed during targeted imaging, late stage OVCA (n = 16 hens including 7 serous, 6 endometrioid, 3 mucinous) was associated with moderate to profuse ascites and metastasized to peritoneal and abdominal organs. Tumors in early stage OVCA (n = 7 including 4 serous, 2 endometrioid, 1mucinous) were limited to the ovary with no or little ascites.

Overall, mean signal intensity (mean ± SD) of IL-16-targeted imaging in normal healthy hens with low egg laying rates was $27.7 \times 10^5 \pm 3.3 \times 10^5$ which was 1.06 fold higher than the pre-contrast signal intensities (**Figure 3**). However the difference was not statistically significant. On the other hand, compared with pre-contrast ($39.9 \times 10^5 \pm 10.8 \times 10^5$) imaging, the mean signal intensity increased significantly ($P<0.05$) to $61.9 \times 10^5 \pm 21.2 \times 10^5$) in post-contrast imaging in hens with tumor masses limited to the ovary (early stage). Thus, IL-16-targeted contrast enhanced imaging increased ultrasound signal intensity to 1.55 fold in hens with early stage OVCA (**Figure 3**). Similarly, in hens with late stage OVCA, the mean signal intensity (mean ± SD) increased significantly ($P<0.001$) from $50.88 \times 10^5 \pm 10.37 \times 10^5$ in pre-contrast imaging to $67.89 \times 10^5 + 10.86 \times 10^5$) in post-contrast imaging (**Figure 3**). Pre-as well as post-contrast ultrasound signal intensities did not differ significantly among different histological sub-types of ovarian tumors.

3.2. Immunohistochemical detection of IL-16 expressing cells and microvessels. IL-16-expressing cells were detected in the stroma of normal or tumor-bearing ovaries and in the tumor vicinity including spaces between tumor glands (**Figure 4, top panel**). A number of epithelial cells (not all) in normal or tumor glands were also positive for IL-16 (**Figure 4, top panel B & C)**.Very few IL-16-expressing cells were seen in the ovarian stroma and the follicular theca layer of normal healthy hens with low egg laying rates (**Figure 4, top panel A)**. Compared with normal hens many IL-16-expressing cells were localized in hens with OVCA (**Figure 4, top panel B-C**). The frequency of stromal IL-16 expressing cells was significantly ($P<0.0001$) higher in hens with early stage OVCA (mean ± SD= 21.85 ± 5.42 in 20,000$\mu m^2$of tumor tissue) than in normal hens (9.56 ± 4.87 in 20,000 μm^2 of ovarian stromal tissue), and increased further

in hens with late stage of OVCA (28.56 ± 5.08 in 20,000 μm^2 of tumor tissue) (**Figure 4, bottom panel**).

IL-16-expressing microvessels were detected in both normal ovaries and ovaries with tumor **(Figure 5, top panel A-C)**. In normal ovaries, very few IL-16-expressing microvessels were seen in ovarian stroma (**Figure 5, top panel A**). Compared with normal ovary, many IL-16-expressing microvessels were localized in the stroma of ovaries with tumor (**Figure 5, top panel B-C**). The frequencies of IL-16-expressing microvessels were significantly ($P<0.0001$) greater in hens with early stage OVCA (mean ± SD= 7.0 ± 1.29 in 20,000μm^2 of tumor tissue) than in normal hens (1.71 ± 0.49 in 20,000μm^2 of ovarian stromal tissue) and increased further ($P<0.0001$) in hens with late stage of OVCA (10.33 ± 2.38 in 20,000μm^2 of tumor tissue) (**Figure 5, bottom panel**). Differences in the frequencies of IL-6-expressing microvessels were not observed among different histological sub-types of malignant ovarian tumors in hens.

Increases in signal intensities due to IL-16-targeted contrast imaging were positively correlated with the frequencies of IL-16-expressing microvessels in ovarian tumors at early stage ($r = 0.46$) and late stage ($r = 0.70$). These results support the predictions of IL-16-targeted contrast imaging that enhanced signal intensity due to the contrast imaging in hens with tumors were due to the increased IL-16-expressing cells and microvessels in the ovaries with tumors.

4. **Discussion**

This study examined, for the first time, suitability of IL-16-targeted contrast agent, a newly developed ultrasound imaging agent, in improving the *in vivo* visualization of ovarian tumors in laying hens, a preclinical model of spontaneous OVCA. The results of this study demonstrated

that IL-16-targeted contrast imaging agents bounded with their targets expressed by ovarian tumors at early and late stages in hens and enhanced the intensities of ultrasound imaging signals from these tumors.

Increased expression of IL-16, a proinflammatory cytokine, has been reported to be associated with the development and progression of several malignancies including OVCA [14, 15, 31]. In addition to stromal cells of the tumor, tumor epithelium has also been reported to express IL-16 [14, 15]. Thus IL-16-expressing cells in ovarian tumors represent a potential target for ultrasound imaging for non-invasive detection of OVCA at early stage provided a targeted imaging agent is developed. In this study, compared with pre-contrast, IL-16-targeted contrast enhanced imaging increased the ultrasound signal intensity remarkably both from hens with ovarian tumors at early and late stages. These results suggest that IL-16-targeted contrast agents bounded with their targets in the tumor tissues. In addition, as reported earlier for humans and hens [14, 15], this study also showed significant increase in the frequency of IL-16-expressing cells in hens with early and late OVCA than normal hens. Thus, higher signal intensities in hens with early and late stage OVCA than normal hens may, in part, due to the increased frequency of targets (IL-16-expressing cells) in OVCA hens bounded with their ligands (IL-16-targeted imaging agents).

IL-16 is a proangiogenic factor suggested to stimulate tumor-associated angiogenesis [16]. Furthermore, the frequency of IL-16-expressing cells was reported to be positively correlated with the frequencies of smooth muscle actin (SMA)-expressing microvessels [14] during OVCA development and progression in hens. In this study, endothelial cells of microvessels expressed IL-16. Furthermore, this study also showed that the density of IL-16-

expressing microvessels increased significantly with the development of OVCA and increased further as the tumor progressed to late stages. The frequencies of tumor associated microvessels expressing $\alpha_v\beta_3$-integrins and VEGFR-2 have also been suggested to increase contrast enhanced ultrasound signal intensities [32, 33]. Thus, in addition to malignant cells, increase in the frequency of IL-16-expressing microvessel might also be a reason for the increased signal intensities during contrast enhanced imaging in hens with OVCA.

The results observed in the current study have, from translational point of view, some exceptional aspects. *First*, most of the contrast agents so far developed including two most extensively studies agents $\alpha_v\beta_3$-integrins and VEGFR-2, have limited success as expression of these targets were mainly limited to the blood vessels. Moreover, no corresponding serum markers of these imaging targets specific to OVCA have been established making their application difficult for early detection of OVCA. In contrast, in addition to the expression of IL-16 by the tumor epithelium and the microvessels, IL-16 is also secreted into the circulation. Serum levels of IL-16 have been reported to be increased significantly in association with OVCA development and progression [14, 15]. Thus, serum IL-16 levels offers a potential marker to be used in conjunction with IL-16-targeted contrast enhanced ultrasound imaging for the detection of OVCA at early stage. *Second*, most of the previous studies used rodent models with induced tumors. On the other hand, this study used laying hens, the only widely available and easily accessible spontaneous model of OVCA. Rodents do not develop OVCA spontaneously and the histopathology of induced OVCA is not similar to those of spontaneous OVCA. Moreover, anatomical differences in the location of induced rodent models (subcutaneous tumor) compared with deeper tissue like the ovary may also affect on the transduction of ultrasound signals as well as the behavior of contrast agents. Thus information on the binding ability and detection of

spontaneous OVCA by contrast agents (as seen for IL-16) is essential. *Third*, chickens are easy to access to test and develop targeted imaging agents as well as anti-OVCA drugs for the detection and treatment of spontaneous OVCA. Moreover, because of the lower cost of hens, this model is also suitable for toxicological studies of newly developed imaging agent or therapeutic in a cost-effective way. Presently, studies with hens are ongoing in which animals are being monitored prospectively with IL-16-targeted contrast agents together with serum IL-16 levels to detect spontaneous ovarian tumor development at relatively earlier stages. This study has also some limitations. We did not use animals with benign ovarian tumors. Small sample size specially the number of hens with ovarian tumors may also be a limitation of this study.

5. Conclusion. Overall, the results of the present study suggest that the IL-16-targeted contrast agents bind with their targets expressed by the spontaneous ovarian tumors in hens and enhance the visualization of tumors at early and late stages. This study also suggests that laying hens offer a new avenue for testing and development of new contrast agents and targeted anti-angiogenic therapeutics.

Conflict of interest

The authors declare no conflict of interest

Acknowledgements

This study was supported by the Department of Defense pilot award # W81XWH-12-1-0460 on ovarian cancer. We thank Chet and Pam Utterback, Shelby P Reed, staff of the University of Illinois at Urbana-Champaign Poultry Research Farm, for maintenance of the hens.

References

[1] American Cancer Society (2013). "Cancer Facts & Figures 2013" http://www.cancer.org/research/cancerfactsstatistics/cancerfactsfigures2013/index.

[2] R. Siegel, J. Ma, Z. Zou, A. Jemal, "Cancer statistics, 2014." *CA: A Cancer Journal for Clinicians*, vol. 64, no. 1, pp. 9-29, 2014.

[3] U. Menon, M. Griffin, and A. Gentry-Maharaj, "Ovarian cancer screening--current status, future directions," *Gynecologic Oncology*, vol. 132, no. 2, pp. 490-495, 2014.

[4] S. S. Buys, E. Partridge, A. Black et al., (2011). "Effect of screening on ovarian cancer mortality: the Prostate, Lung, Colorectal and Ovarian (PLCO) Cancer Screening Randomized Controlled Trial," *Journal of American Medical Association*, vol. 305, no. 22, pp. 2295-2303, 2011.

[5] J. S. Abramowicz, "Ultrasonographic contrast media: has the time come in obstetrics and gynecology?" *Journal of Ultrasound in Medicine*, vol. 24, no. 4, pp. 517-531, 2005.

[6] S. Dutta, F. Q. Wang, A. C. Fleischer and D. A. Fishman, "New frontiers for ovarian cancer risk evaluation: proteomics and contrast-enhanced ultrasound." *AJR, American Journal of Roentgenology*, vol. 194, no. 2, pp. 349-354, 2010.

[7] A. C. Fleischer, A. Lyshchik, R. F. Andreotti et al., "Advances in sonographic detection of ovarian cancer: depiction of tumor neovascularity with microbubbles," *AJR, American Journal of Roentgenology*, vol. 194, no. 2, pp. 343-348, 2010.

[8] A. C. Fleischer, A. Lyshchik, H. W. Jones, 3rd et al., "Diagnostic parameters to differentiate benign from malignant ovarian masses with contrast-enhanced transvaginal sonography," *Journal of Ultrasound in Medicine, vol.* 28, no. 10, pp. 1273-1280, 2009.

412 [9] A. C. Fleischer, A. Lyshchik, H. W. Jones, Jr. et al., "Contrast-enhanced transvaginal
413 sonography of benign versus malignant ovarian masses: preliminary findings." *Journal*
414 *Ultrasound in Medicine*, vol. 27, no. 7, pp.1011-1018; quiz 1019-21, 2008.
415 [10] C. R. Anderson, J. J. Rychak, M. Backer et al., "scVEGF microbubble ultrasound contrast
416 agents: a novel probe for ultrasound molecular imaging of tumor angiogenesis," *Investigative*
417 *Radiology*, vol. 45, no. 10, pp. 579-585, 2010.
418 [11] J. K. Willmann, R. Paulmurugan, K. Chen et al., "US imaging of tumor angiogenesis with
419 microbubbles targeted to vascular endothelial growth factor receptor type 2 in mice." *Radiology*,
420 vol. 246, no. 2, pp. 508-518, 2008.
421 [12] A. Maccio and C. Madeddu, "Inflammation and ovarian cancer," *Cytokine*, vol. 58, no. 2,
422 pp. 133-147, 2012.
423 [13] W. Cruikshank, H. Kornfeld and D. M. Center. "Interleukin-16," *Journal of Leukocyte*
424 *Biology*, vol. 67, no. 6, pp. 757-766, 2000.
425 [14] A. Yellapa, J. M. Bahr, P. Bitterman et al., "Association of interleukin 16 with the
426 development of ovarian tumor and tumor-associated neoangiogenesis in laying hen model of
427 spontaneous ovarian cancer," *International Journal of Gynecological Cancer*, vol. 22, no. 2,
428 pp.199-207, 2012.
429 [15] A. Yellapa, P. Bitterman, S. Sharma et al., "Interleukin 16 expression changes in association
430 with ovarian malignant transformation," *American Journal of Obstetrics and Gynecology*, vol.
431 210, no. 3, pp. 272 e1-10, 2014.
432 [16] N. L. Mathy, W. Scheuer, M. Lanzendorfer et al.,"Interleukin-16 stimulates the expression
433 and production of pro-inflammatory cytokines by human monocytes," *Immunology*, vol. 100, no.
434 1, pp. 63-69, 2000.

[17] D. J. Lee, A. Lyshchik, J. Huamani et al., "Relationship between retention of a vascular endothelial growth factor receptor 2 (VEGFR2)-targeted ultrasonographic contrast agent and the level of VEGFR2 expression in an in vivo breast cancer model," *Journal of ultrasound in Medicine*, vol. 27, no. 6, pp. 855-866, 2008.

[18] A. Lyshchik, A. C. Fleischer, J. Huamani et al., "Molecular imaging of vascular endothelial growth factor receptor 2 expression using targeted contrast-enhanced high-frequency ultrasonography," *Journal of Ultrasound in Medicine*, vol. 26, no. 11, pp. 1575-1586, 2007.

[19] J. K. Willmann, A. M. Lutz, R. Paulmurugan et al., "Dual-targeted contrast agent for US assessment of tumor angiogenesis in vivo," *Radiology*, vol. 248, no. 3, pp. 936-944, 2008.

[20] C. Rodriguez-Burford, M. N. Barnes, W. Berry, et al., "Immunohistochemical expression of molecular markers in an avian model: a potential model for preclinical evaluation of agents for ovarian cancer chemoprevention" *Gynecologic Oncology*, vol. 81, no. 3, pp. 373-379, 2001.

[21] A. Barua, P. Bitterman, J. S. Abramowicz, et al., "Histopathology of ovarian tumors in laying hens: a preclinical model of human ovarian cancer," *International Journal of Gynecological Cancer*, vol. 19, no. 4, pp. 531-539, 2009.

[22] Fredrickson, T. N. (1987), "Ovarian tumors of the hen," *Environmental Health Perspectives*, vol 73, no. 1: 35-51.

[23] E. Jackson, K. Anderson, C. Ashwell et al., (2007), "CA125 expression in spontaneous ovarian adenocarcinomas from laying hens," *Gynecologic Oncology*, vol. 104, no. 1, pp. 192-198, 2007.

[24] K. Stammer, S. L. Edassery, A. Barua et al., "Selenium-Binding Protein 1 expression in ovaries and ovarian tumors in the laying hen, a spontaneous model of human ovarian cancer," *Gynecologic Oncology*, vol. 109, no. 1, pp. 115-121, 2008.

[25] J. R. Giles, H. L. Shivaprasad and P. A. Johnson, "Ovarian tumor expression of an oviductal protein in the hen: a model for human serous ovarian adenocarcinoma," *Gynecologic Oncology*, vol. 95, no. 3, pp. 530-533, 2004.

[26] M. F. Khan, J. M. Bahr, A. Yellapa et al., "Expression of Leukocyte Inhibitory Immunoglobulin-like Transcript 3 Receptors by Ovarian Tumors in Laying Hen Model of Spontaneous Ovarian Cancer," *Translational Oncology*, vol. 5, no. 2, pp. 85-91, 2012.

[27] A. Barua, J. S. Abramowicz, J. M. Bahr et al., "Detection of ovarian tumors in chicken by sonography: a step toward early diagnosis in humans?" *Journal Ultrasound in Medicine*, vol. 26, no. 7, 909-919.

[28] A. Barua, P. Bitterman, J. M. Bahr et al., "Detection of tumor-associated neoangiogenesis by Doppler ultrasonography during early-stage ovarian cancer in laying hens: a preclinical model of human spontaneous ovarian cancer," *Journal Ultrasound in Medicine*, vol. 29, no. 2, pp. 173-182, 2010.

[29] Barua, A., P. Bitterman, J. M. Bahr, et al., "Contrast-enhanced sonography depicts spontaneous ovarian cancer at early stages in a preclinical animal model," *Journal Ultrasound in Medicine*, vol. 30, no. 3, pp. 333-345, 2011.

[30] A. Barua, A. Yellapa, J. M. Bahr et al., "Expression of death receptor 6 by ovarian tumors in laying hens, a preclinical model of spontaneous ovarian cancer," *Translational Oncology*, vol, 5, no. 4, pp. 260-268, 2012.

[31] J. Richmond, M. Tuzova, W. Cruikshank and D. Center, "Regulation of cellular processes by interleukin-16 in homeostasis and cancer," *Journal of Cellular Physiology*, vol. 229, no. 2, pp. 139-147, 2014.

[32] A. Barua, A. Yellapa, J. M. Bahr et al., "Enhancement of ovarian tumor detection with alphavbeta3 integrin-targeted ultrasound molecular imaging agent in laying hens: a preclinical model of spontaneous ovarian cancer," *International Journal Gynecological Cancer*, vol. 24, no. 1, pp. 19-28, 2014.

[33] A. Barua, T. Qureshi, P. Bitterman et al., "Molecular targeted imaging of vascular endothelial growth factor receptor (VEGFR)-2 and anti-NMP autoantibodies detect ovarian tumor at early stage," *Cancer Research*: April 15, 2012; Vol.72, no. 8, Supplement 1, Abstract nr 2455, 2012.

FIGURE LEGENDS

FIGURE 1: Enhancement of signal intensity of ultrasound imaging of hen ovarian tumors by IL-16-targeted contrast agents. A) Case 1: Pre-contrast gray scale ultrasonogram of a hen ovary showing solid mass (dotted lines) with septa and accompanied ascites (AS). B) Post-contrast gray scale ovarian sonogram of the same hen showing enhanced visualization of the solid tumor mass. C) Case-2: Pre-contrast gray scale sonogram depicting a suspected ovarian mass (dotted lines) in another hen. D) Gray scale sonogram of the same ovary (shown in C), depicting solid tumor mass with enhanced signal intensity after the injection of targeted imaging agents. E) Gross presentation confirmed the imaging prediction of an ovarian tumor (shown in C-D, appeared as cauliflower –shaped, yellow circled). F) Histological examination showed a serous malignant tumor with cells containing large pleomorphic nuclei surrounded by a sheath of fibromuscular tissues. H & E staining.

FIGURE 2: Detection of spontaneous ovarian tumors at early stage in hens by IL-16-targeted contrast enhanced ultrasound imaging. A) Pre-contrast ovarian sonogram showing low intensity of ultrasound imaging. Presence of tumor-related solid mass in the ovary is inconclusive. B-C) Corresponding contrast enhanced sonogram with enhanced visualization of ultrasound imaging at 5min and 7min after the injection of contrast agents, respectively, suggesting the presence of a small solid mass (yellow dotted lines) in the ovary. D) Gross morphology shows the presence of a tissue mass (yellow dotted line) limited to a part of the ovary accompanied with a little ascites.

FIGURE 3: Changes in the signal intensity of ultrasound imaging by IL-16-targeted contrast agent in the ovary of laying hens with or without ovarian cancer (OVCA). Compared with pre-contrast imaging, IL-16-targeted contrast agents enhanced the intensities of ultrasound imaging

significantly in hens with early stage OVCA as well as in late stage OVCA. However, significant differences were not observed between the pre- and post-contrast imaging in healthy hens. Different letters denote significant differences in the intensities of ultrasound imaging between the pre- contrast and post-contrast imaging within the same group including hens with normal ovaries and with early and late stages of OVCA.

FIGURE 4: Immunohistochemical localization of IL-16-expressing cells in the ovaries of hens predicted to be normal or cancerous by IL-16-targeted contrast enhanced ultrasound imaging. ***Top panel***: A) Section of a normal hen ovary showing few IL-16 expressing cells in the ovarian stroma (S) and the follicular (F) theca (T). B-C) Sections of tumor ovaries at early (B) and late (C) stages of OVCA. Compared with normal ovary, many IL-16 expressing cells are seen in OVCA hens. S= stroma, Arrows indicate the examples of IL-16 expressing cells. ***Bottom panel:*** Compared with normal, the frequency of IL-16 expressing cells increased significantly (P<0.001) with tumor development and progression to late stages. Bars with different letters indicate significant differences in the frequencies of IL-16-expressing cells among hens with normal, early stage and late stage OVCA.

FIGURE 5: Expression of IL-16 by microvessels in the ovaries of hens with or without ovarian tumors scanned by targeted ultrasound imaging. Top panel: A) Section of a normal ovary showing few IL-16-expressing microvessels in the stroma (S). B and C) Sections of malignant ovaries at early (B) and late (C) stages of OVCA. Compared with normal (A), more IL-16-expressing microvessels are seen in OVCA hens. S= stroma, Arrows indicate examples of IL-16 –expressing microvessels vessels. ***Bottom panel:*** Compared with normal, the frequency of IL-16-expressing microvessels was significantly (P<0.001) high in OVCA hens at early and late

547 stages. Bars with different letters indicate significant differences in the frequencies of IL-16-

548 expressing microvessels among hens with normal, early stage and late stage OVCA.

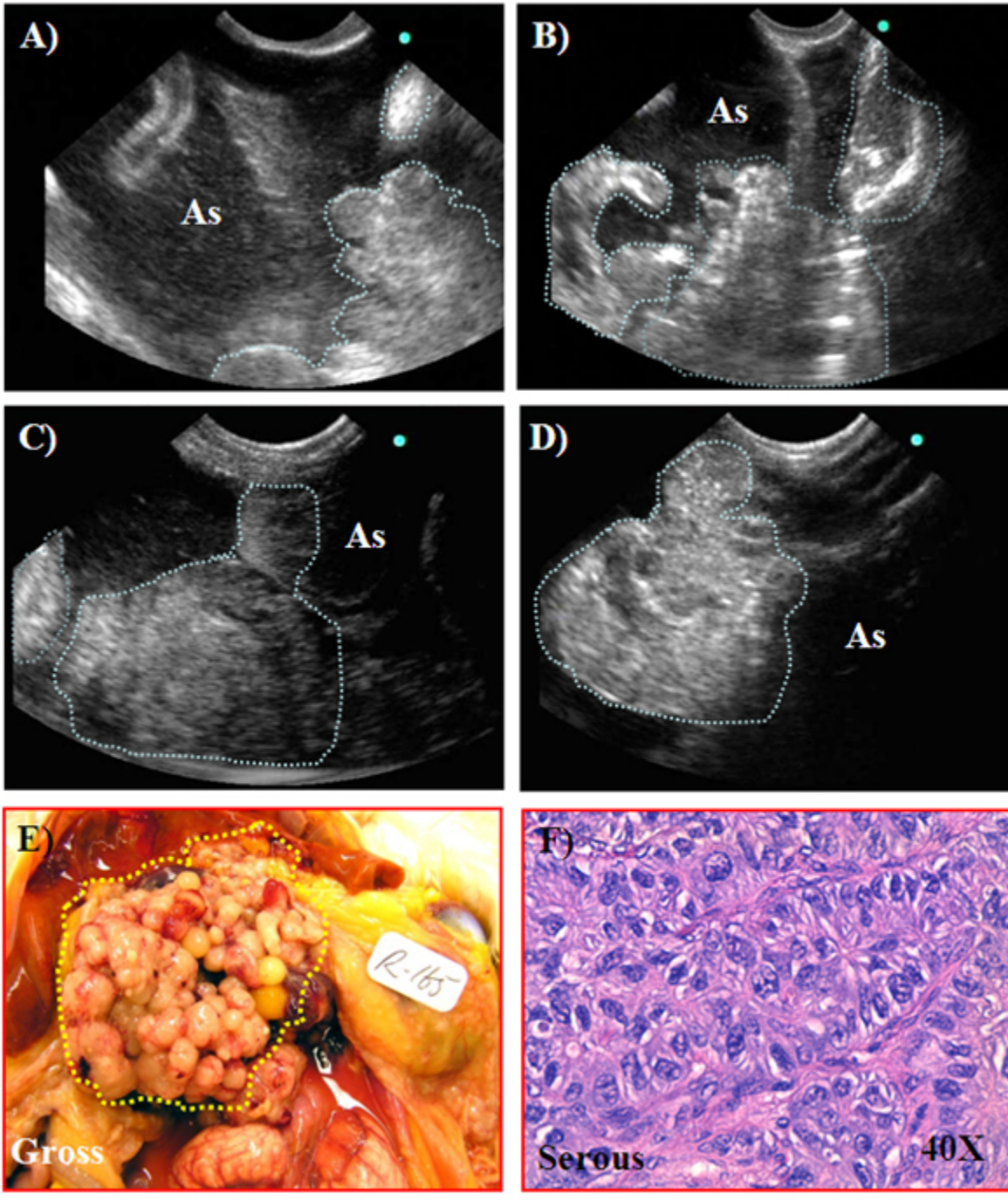

FIGURE 1

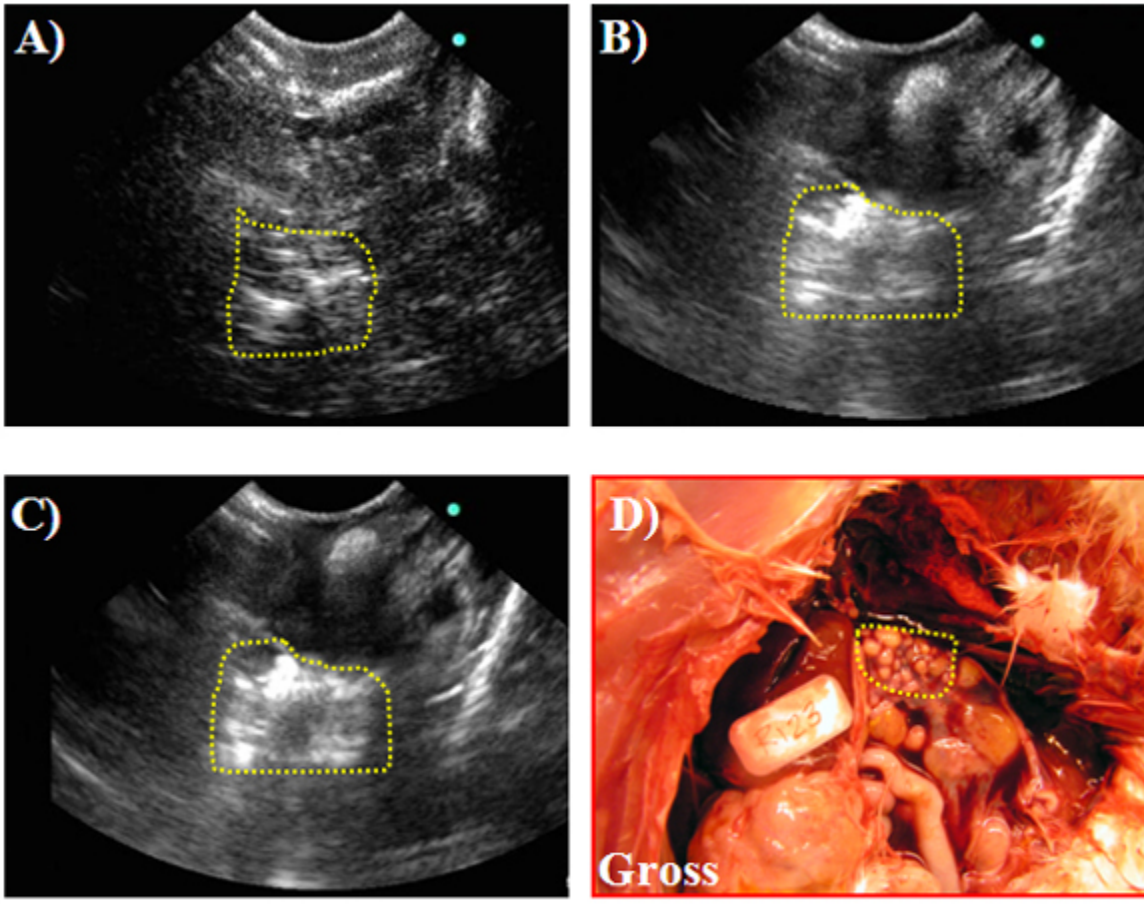

FIGURE 2

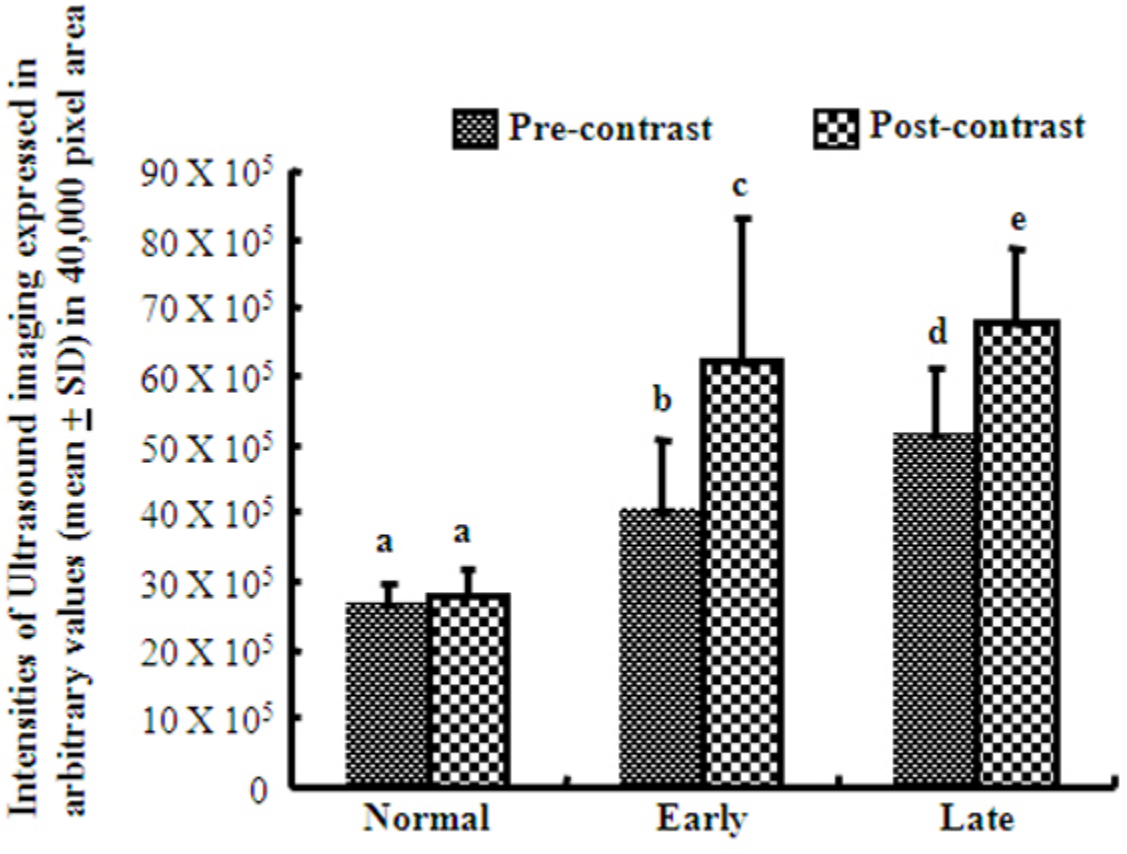
Intensities of Ultrasound imaging expressed in arbitrary values (mean ± SD) in 40,000 pixel area
Pre-contrast
Post-contrast
90 X 10^5
80 X 10^5
70 X 10^5
60 X 10^5
50 X 10^5
40 X 10^5
30 X 10^5
20 X 10^5
10 X 10^5
0
a
a
b
c
d
e
Normal
Early
Late

FIGURE 3

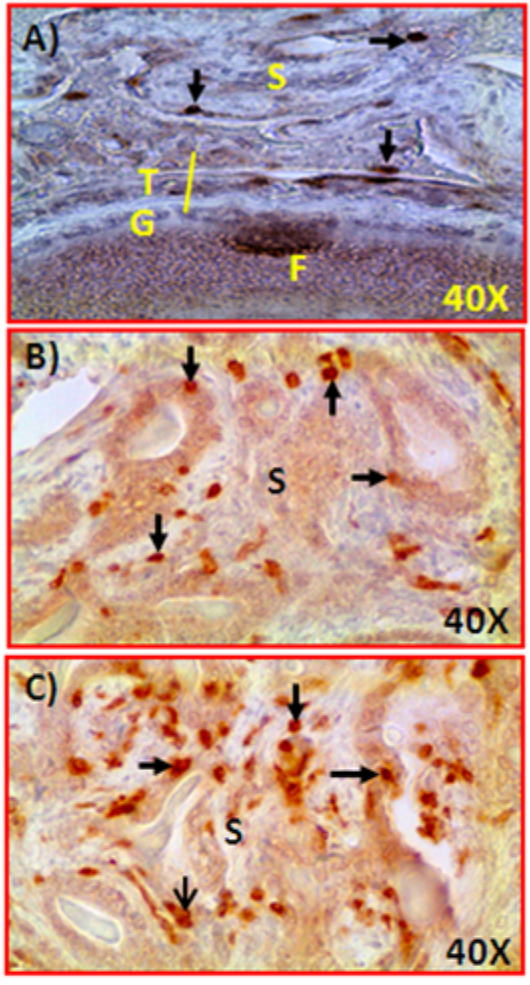
A)
S
T
G
F
40X
B)
S
40X
C)
S
40X

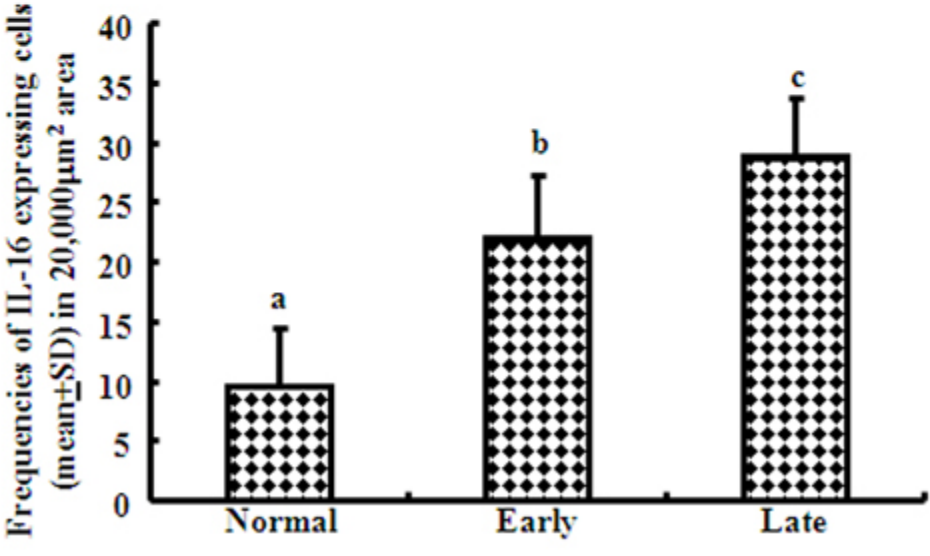
Frequencies of IL-16 expressing cells (mean±SD) in 20,000µm² area
40
35
30
25
20
15
10
5
0
a
b
c
Normal
Early
Late

FIGURE 4

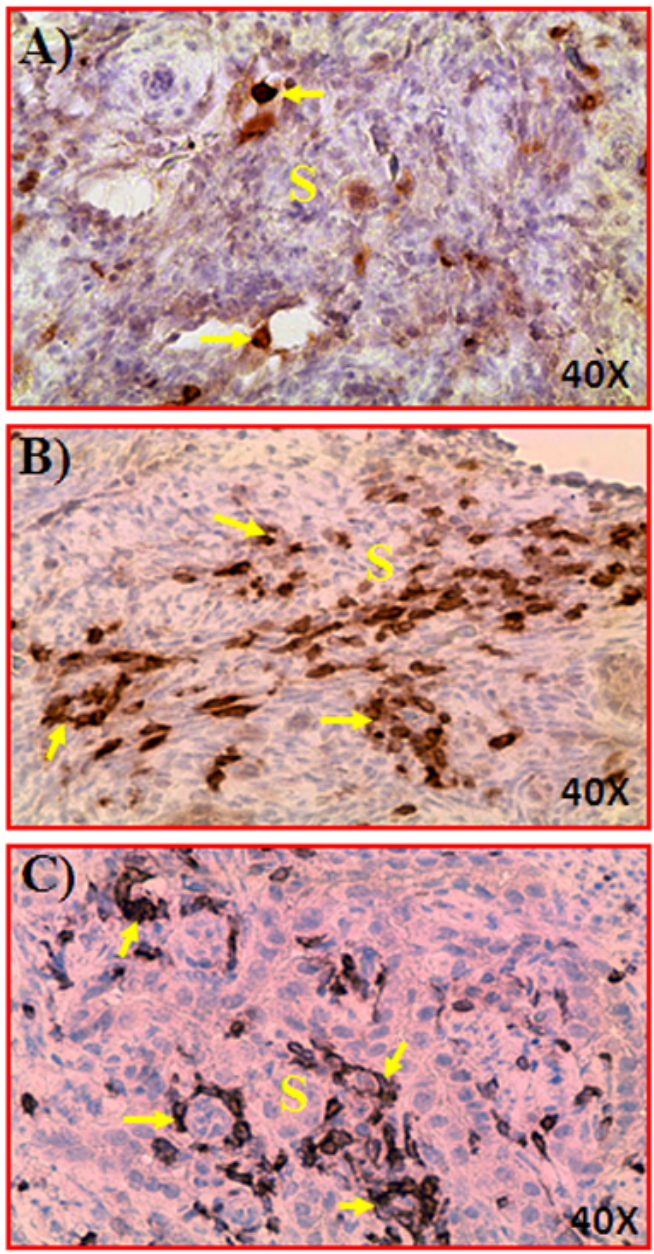
A)
S
40X
B)
S
40X
C)
S
40X

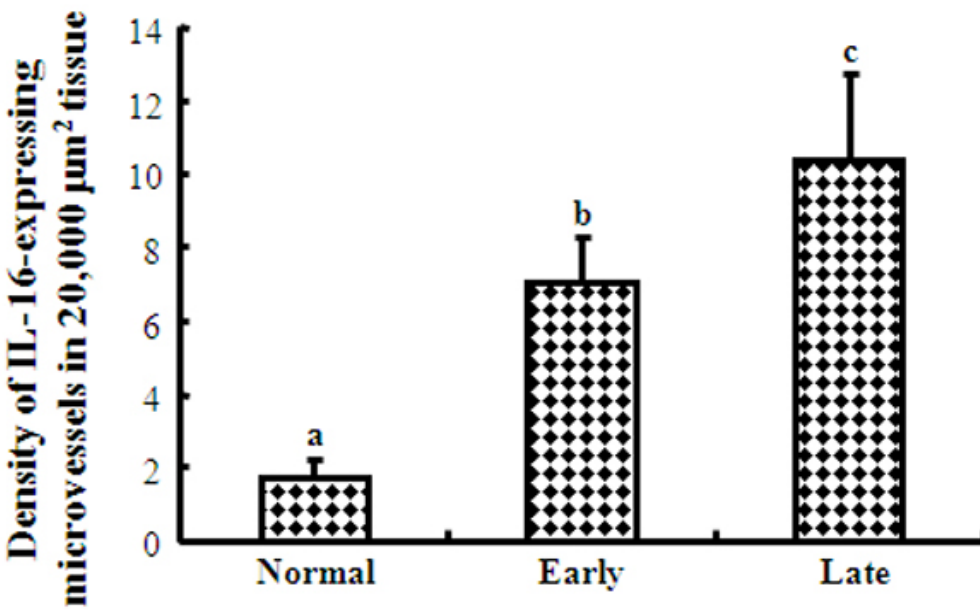
Density of IL-16-expressing microvessels in 20,000 μm² tissue
14
12
10
8
6
4
2
0
a
b
c
Normal
Early
Late

FIGURE 5